

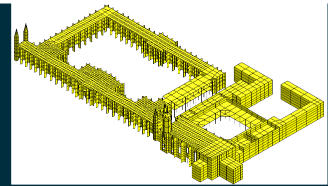

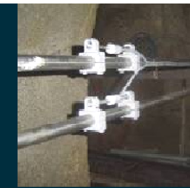
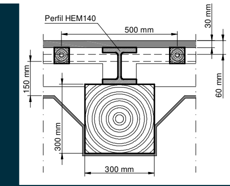

Anisotropic nonlinear homogenized constitutive model of masonry walls

SAHC 2020

Michel Y. Chalhoub

University of Minho

Guimaraes, 2020

University of Minho
University of Padova
Czech Technical University in Prague
Technical University of Catalonia
ARCCHIP- ITAM

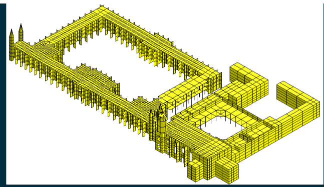

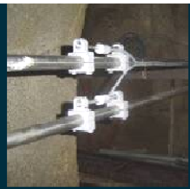

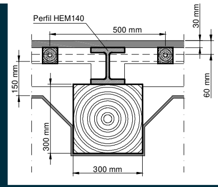

The content of the present document derives from a SAHC master thesis work that belongs to the author and University of Minho. The use of any result should be subjected to a prior approval of the author.

University of Minho
University of Padova

Czech Technical University in Prague
Technical University of Catalonia

ARCCHIP- ITAM

Table of contents

Motivation and scope

Motivation and scope

Structural analysis of URM : complex task especially for irregular or multi-leaf walls. *Why?*

Heterogeneity and (spatial) **variability** of its **mechanical properties**.

Reliable structural analysis ➔ A **proper mechanical characterization of the masonry**.

How?

In-situ non-destructive or minor-destructive tests → acceptable values in the elastic range.

Shear, compressive or tensile strengths → accomplishable via destructive tests.

FE homogenization methods ➔ Special interest, *Why?*

Response of masonry under different loading conditions → **reduction of** undesired **damage.**

Constitute the focus of the present work.

Motivation and scope

Modelling strategies for the mechanical study of masonry structures:

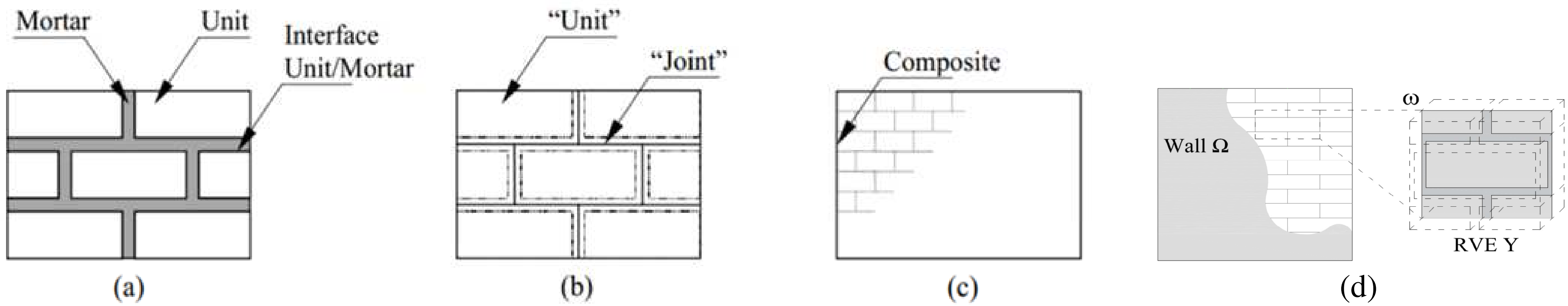

(a) detailed micro-modelling; (b) simplified micro-modelling; (c) macro-modelling; (d) multi-scale method (Silva et al. 2018).

Main objective of the current work:

To develop a FE homogenization-based approach based on a simplified micro-modelling, and to apply it at a multi-scale level.

FE homogenization approach

FE homogenization approach

- Homogenization approach based on some specific types of boundary conditions, as for instance, boundary displacement varying linearly with the position.
- Accuracy of the symmetrical positive-definite compliance tensor in the elastic phase.

Pre-processing phase ad-hoc algorithm

- An *ad-hoc* algorithm has been developed in order to avoid singularities due to the high density of joints.

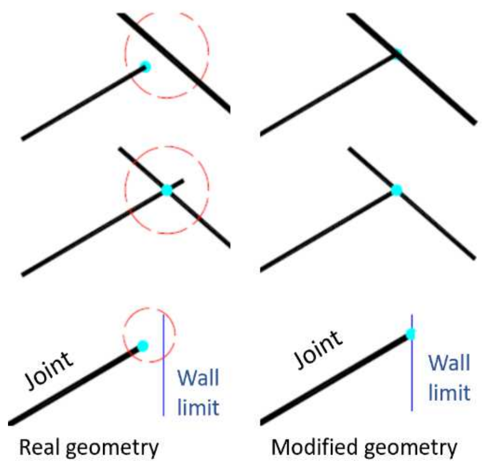

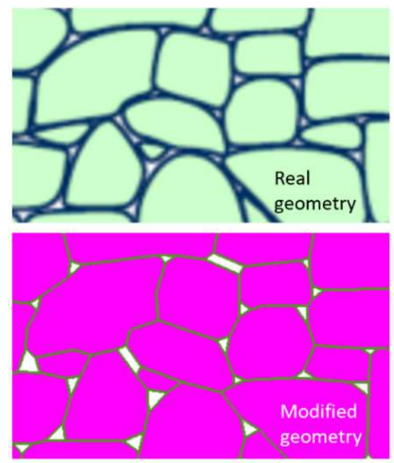

Modifications induced on the geometry of a highly jointed media.

Simplified Micro-model validation

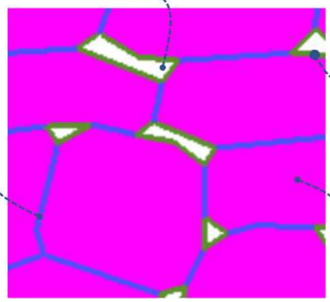

Mechanical constitutive models

Mortar

- Cohesive Fracture with Damage-Plasticity and Unilateral Contact (CZFRAC, Disroc 2020)

Compression
Nonlinear elasticity with maximum closure

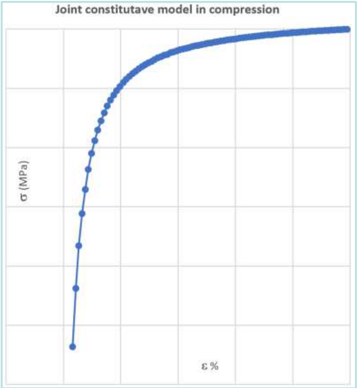

Tension
Plasticity & damage

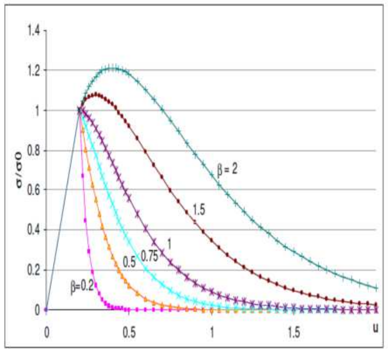

Traction-Separation curves for different b values

Shear
Plasticity & damage

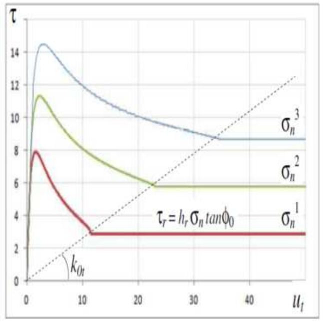

Shear stress versus slip under different compressive normal stresses for the option With plasticity: the curves join and follow the elastic line with residual stiffness k_{0t}

Failure surface
Cohesive joint

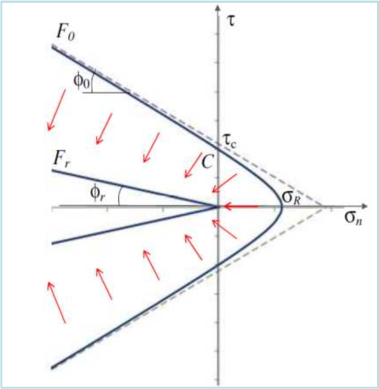

Cohesive Fracture with Damage and Plasticity (CZFRAC, Disroc 2020)

Simplified Micro-model validation

Mechanical constitutive models

Units and thick mortar

- ANELVIP (Disroc 2020): Anisotropic elasto-viscoplastic material : Ellipsoidal elasticity, anisotropic Mohr-Coulomb with cut-off or Drucker-Prager plasticity and Lemaitre creep law.

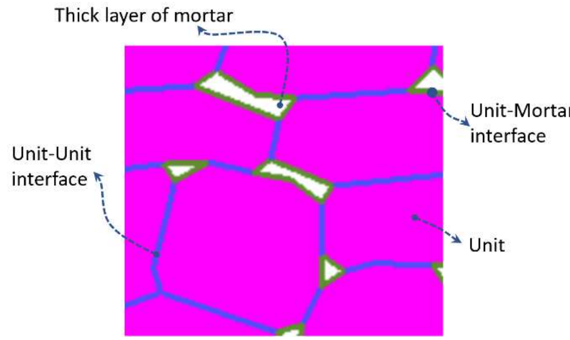

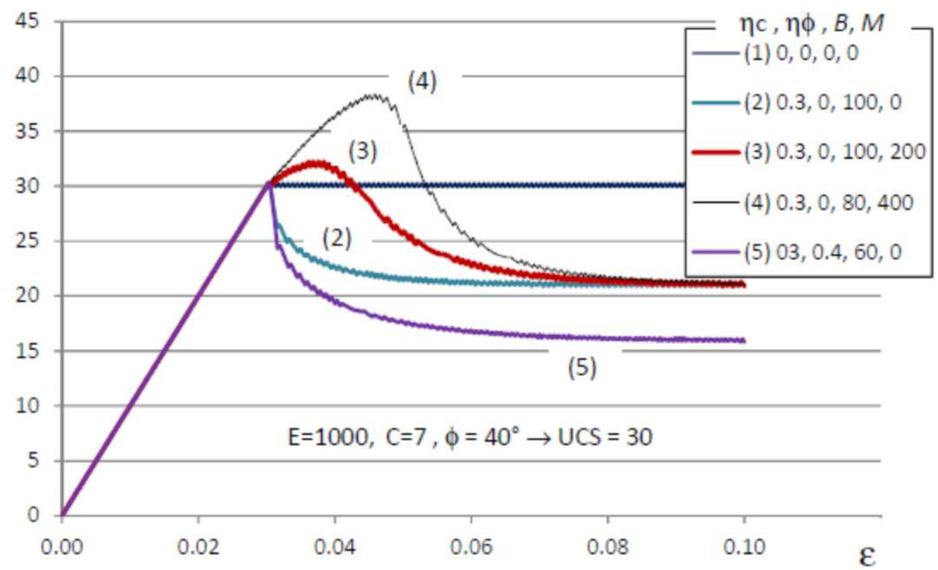

Stress-Strain curves for ANELVIP elastoplastic material with different softening parameters (Disroc 2020).

Simplified Micro-model validation: running bond

Masonry characteristics

Brick units: 210×100×52 mm³. Mortar joints thickness: 10 mm.

E_{brick} = 20,000 MPa; ν_{brick}=0.15; E_{mortar} = E_{brick}/r (1 < r < 1000) and ν_{mortar}= 0.15.

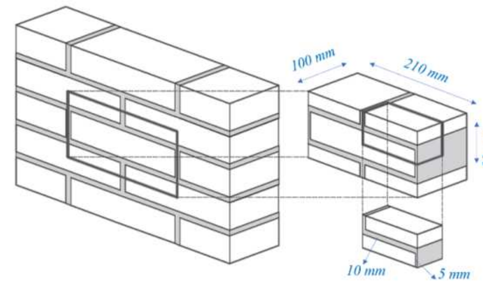

Zucchini and Lourenço (2002)

Homogenized elastic stiffness

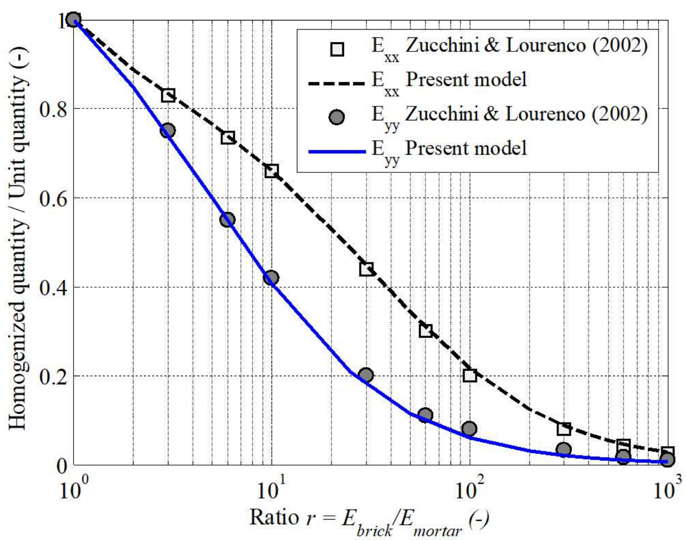

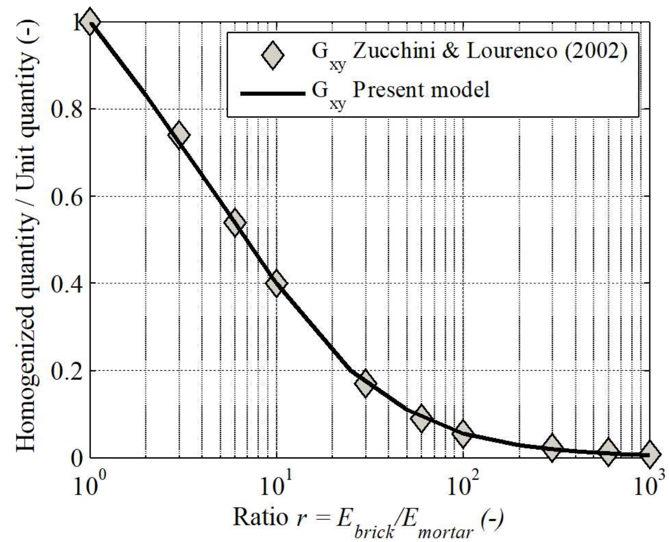

- Results are in good agreement (maximum relative error is below 4.6%).

Simplified Micro-model validation: running bond

Masonry characteristics

$E_{unit} = 20{,}000\ MPa;\ \nu_{unit} = 0.15;\ E_{mortar} = 10{,}000\ MPa,\ f_{cb} = 50\ MPa,\ f_{tb} = 2.5\ MPa,\ f_{cm} = 6\ MPa,\ f_{tm} = 0.6\ MPa,\ \phi = 30\ degrees$.

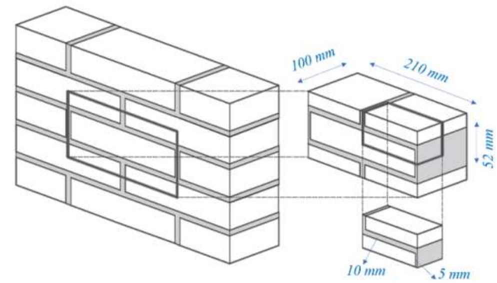

Zucchini and Lourenço (2002)

Inelastic range: in-plane Compression

- Results in compression are concordant:
  - Elastic part.
  - Pick strength.
  - Post-pic behavior.

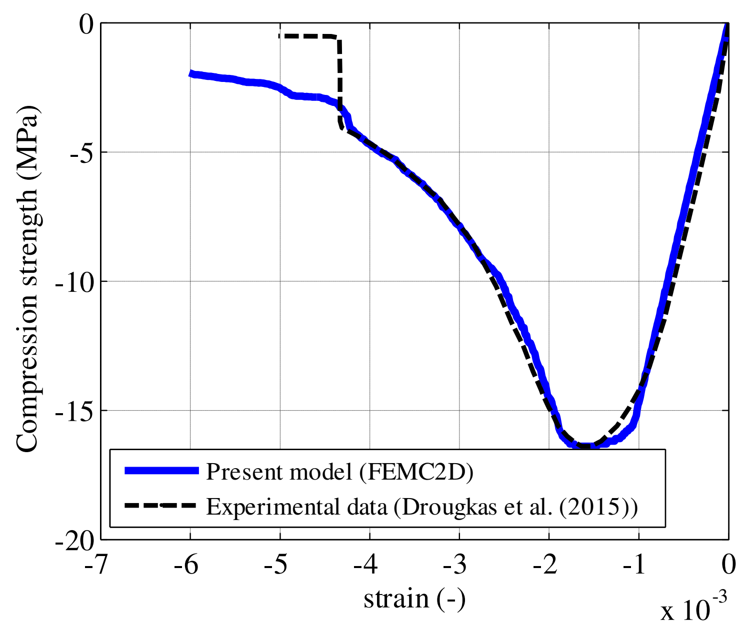

Simplified Micro-model validation: running bond

Masonry characteristics

$E_{unit} = 11{,}000\ MPa\ ,\ \ \nu_{unit} = 0.2\ ,\ \ E_{mortar} = 4{,}000\ MPa\ ,$ $f_{tm} = 0.25\ MPa,\ c = 0.6\ MPa$ (mortar cohesion), and $\phi =$ $30\ degrees$ (mortar friction angle).

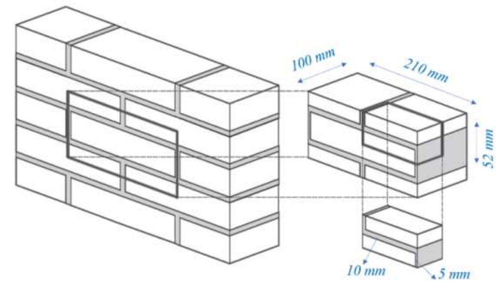

Zucchini and Lourenço (2002)

Inelastic range: Tension and shear, in-plane and out-of-plane validation

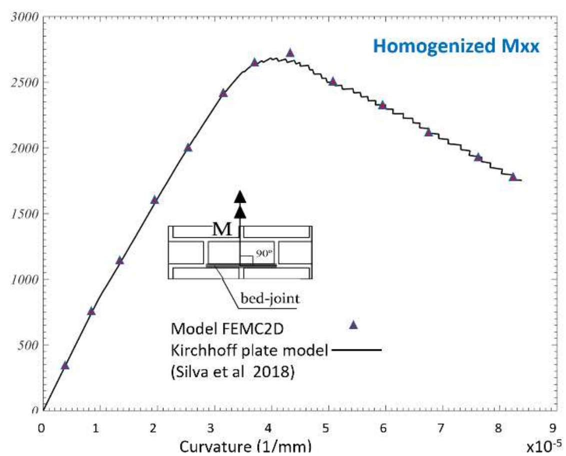

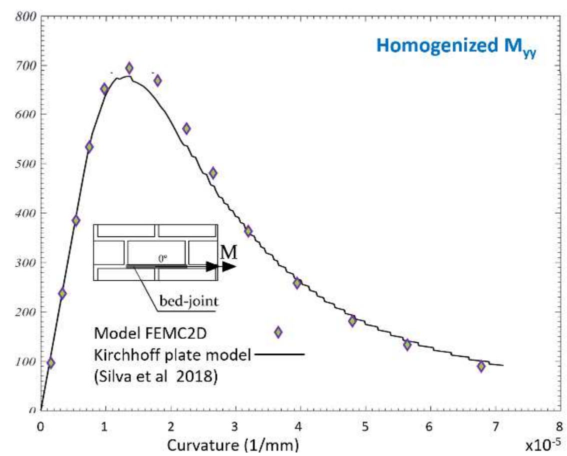

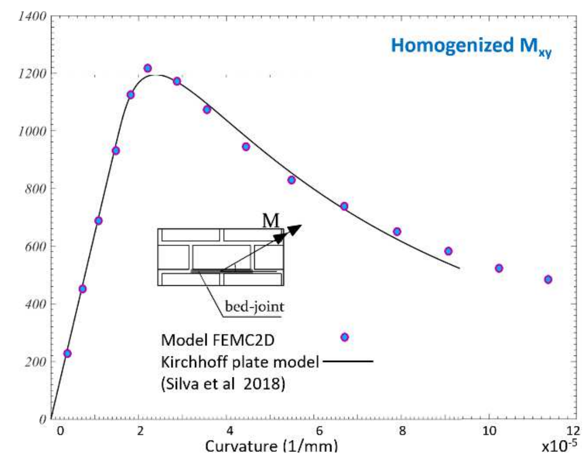

- The model reproduces the orthotropic behavior of the considered panels in terms of moment-curvature curves with acceptable accuracy (maximum difference 5%).

Macro-model validation

Mechanical constitutive models

Same model of units and thick mortar : ANELVIP

Linear elasticity with Saint-Venant ellipsoidal anisotropy

$$\begin{bmatrix} \frac{1}{E_1} & \frac{-\nu}{\sqrt{E_1E_2}} & \frac{-\nu}{\sqrt{E_1E_3}} & & & \\ \frac{-\nu}{\sqrt{E_1E_2}} & \frac{1}{E_2} & \frac{-\nu}{\sqrt{E_2E_3}} & & & \\ \frac{-\nu}{\sqrt{E_1E_3}} & \frac{-\nu}{\sqrt{E_2E_3}} & \frac{1}{E_3} & & & \\ & & & \frac{2(1+\nu)}{\sqrt{E_2E_3}} & & \\ & & & & \frac{2(1+\nu)}{\sqrt{E_1E_3}} & \\ & & & & & \frac{2(1+\nu)}{\sqrt{E_1E_2}} \end{bmatrix}$$

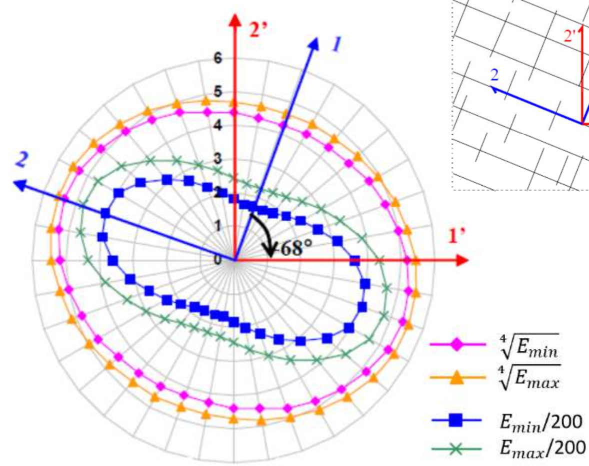

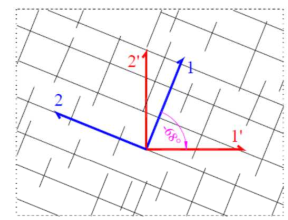

[Chalhoub 2010]

The indicator surface of the Young's modulus fourth root is an ellipsoid: *Parameters: **E1, E2, ν.***

Applications

The numerical simulations presented in the following used the Finite Element code Disroc and its damage and softening plasticity models ANELVIP for bulk materials and CZFRAC for joints (Disroc 2020).

Homogenization of a rubble wall

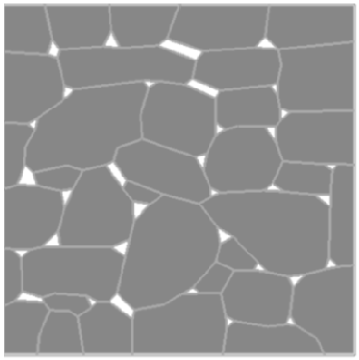

Rubble wall

Geometry and mesh

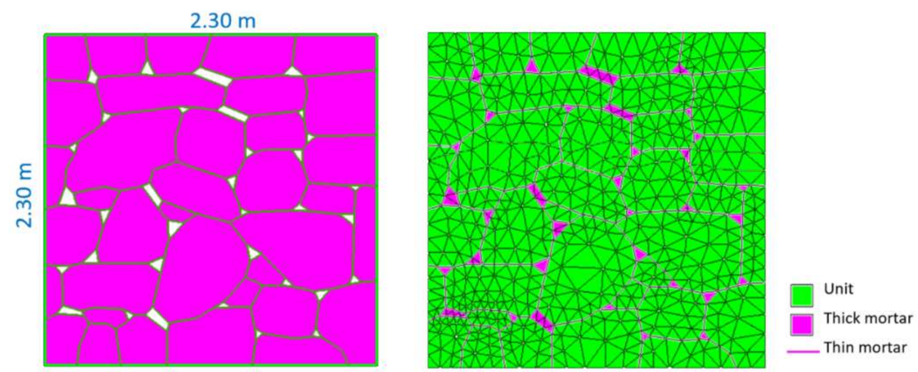

1149 triangular elements and 417 interface elements.

Materials

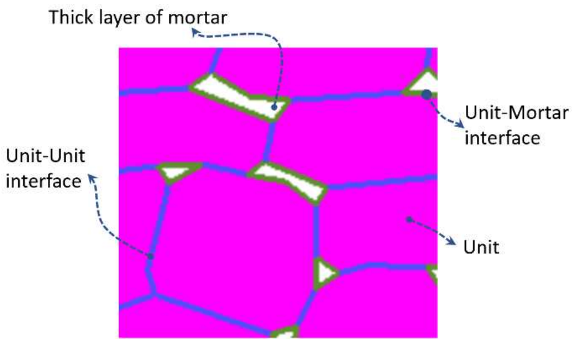

- *Units:* $E_{brick} = 30{,}000\ MPa$; $\nu_{unit} = 0.25$; $f_{cb} = 17\ MPa$, $f_{tb} = 2\ MPa$, $C_b = 5\ MPa$; $\Psi_b = \phi_b = 30\ degrees$; $\eta_c = 0.7$; $\eta_\phi = 0$; $B = 5$; $M = 0$ *(brittle material).*
- *Thin mortar:* $K_n = 25000\ MPa/m$; $K_{0n} = 3000\ MPa/m$; $K_t = 5000\ MPa/m$; $K_{0t} = 1000\ MPa/m$; $c = 0.5\ MPa$; $f_{tm} = 0.5\ MPa$, $\phi = \psi = 25$ degrees; e = 20 mm, $h_r = 1$; $\beta = 1.2$ (slightly brittle).
- *Thick mortar:* $E_{Tm} = 5{,}000\ MPa$; $\nu_{Tmr} = 0.2$; $f_{cTm} = 17\ MPa$, $f_{tm} = 2\ MPa$, $C_{Tm} = 2\ MPa$; $\Phi_{Tm} = \phi_{Tm} = 25$ degrees; $\eta_c = 0.7$; $\eta_\phi = 0$; $B = 70$; $M = 0$ *(brittle material).*

Rubble wall

Boundary conditions

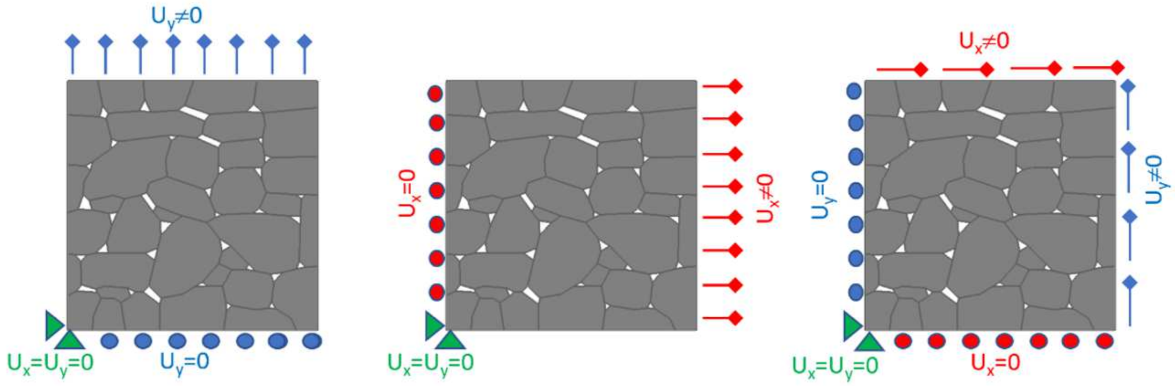

(a) (b) (c)

Imposed displacement on the RVE boundaries:

(a) - Vertical mode-I response, i.e. compression and tension;

(b) - Horizontal mode-I response, i.e. compression and tension;

(c) - Pure shear.

Rubble wall

Framework to derive the composite 2D and 3D failure surfaces:

- **One-step strategy**: boundary conditions applied simultaneously.

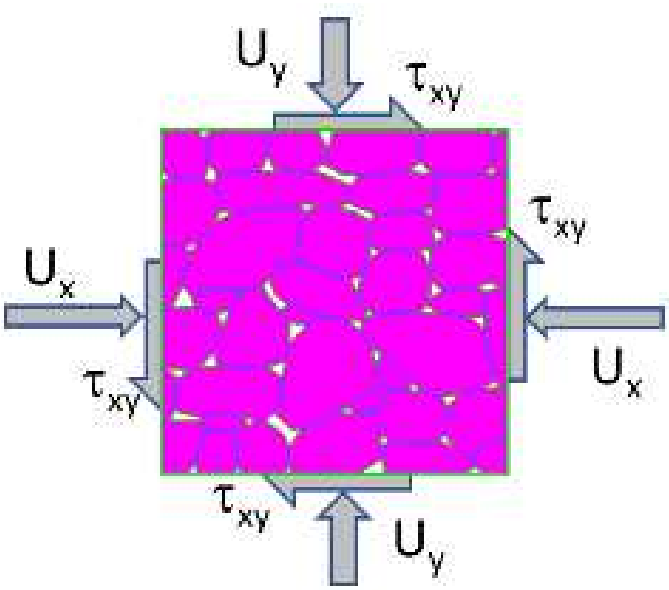

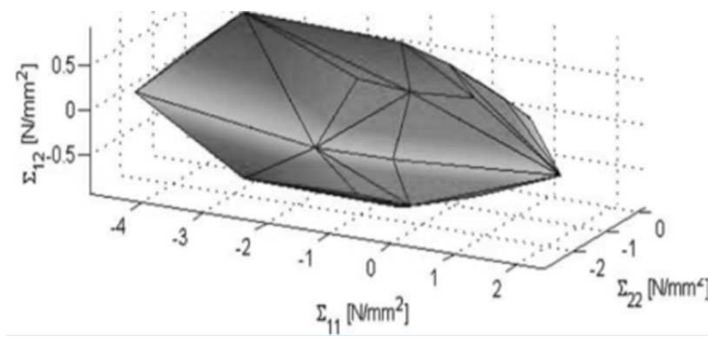

3D failure surfaces

Rubble wall

Framework to derive the composite 2D and 3D failure surfaces:

- **Two-step strategy**: boundary conditions applied in multiple steps.

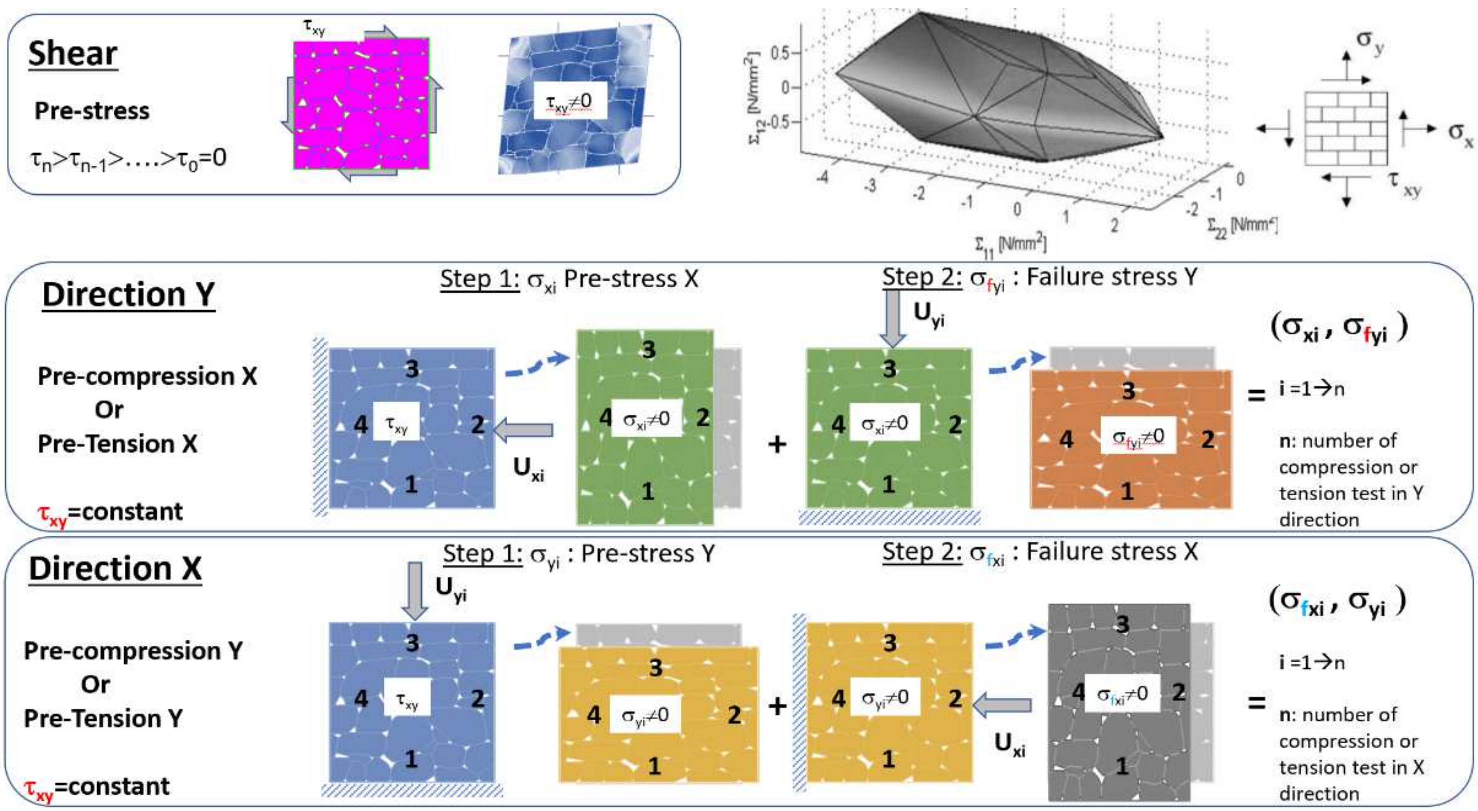

Rubble wall

Micro-Model: Compression test (Two-step approach)

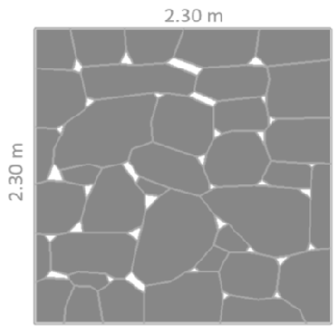

- A slight orthotropic behavior in elasticity.
- Quasi-isotropic behavior in plasticity.
- Compressive strength is governed by the units behavior.

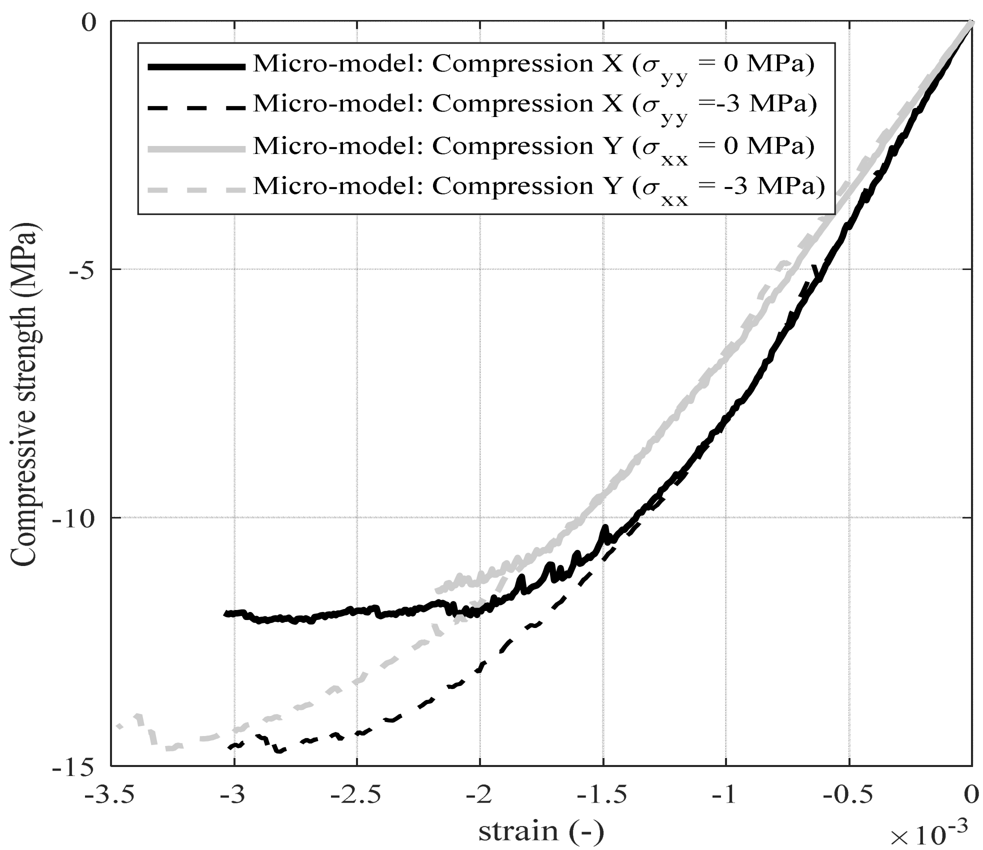

Rubble wall

Micro-Model: Compression test, failure mechanism

(a) normalized total displacement (b) total displacement vectors (c) irreversible strain

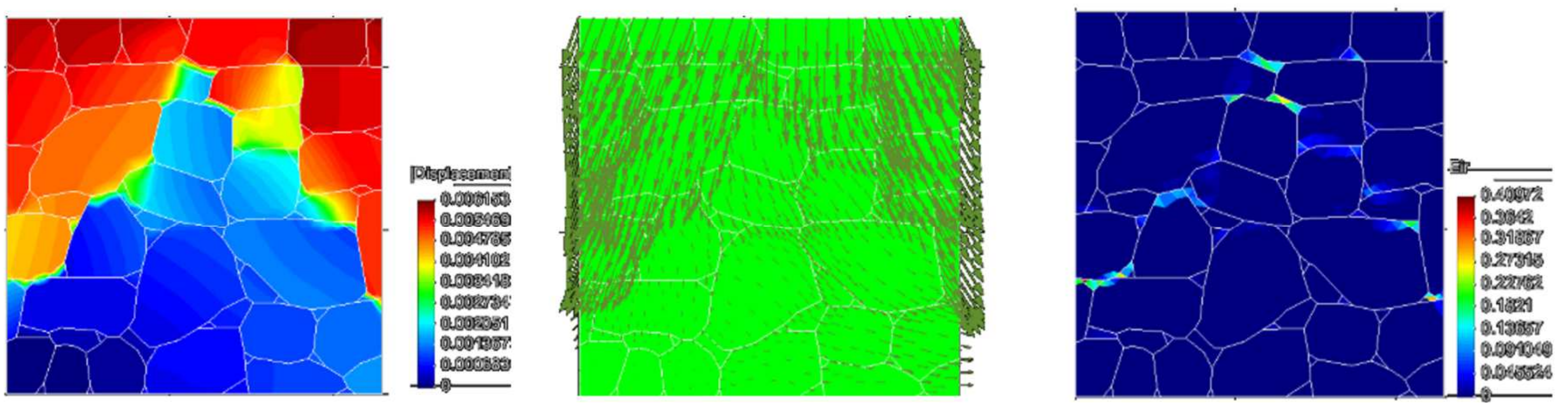

- The micro-model is able to predict the failure mechanism: occurring through a continuous path that connects thick mortar areas (c).

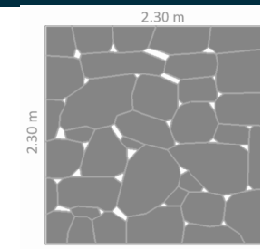

Rubble wall

Micro-Model: Tension and shear tests

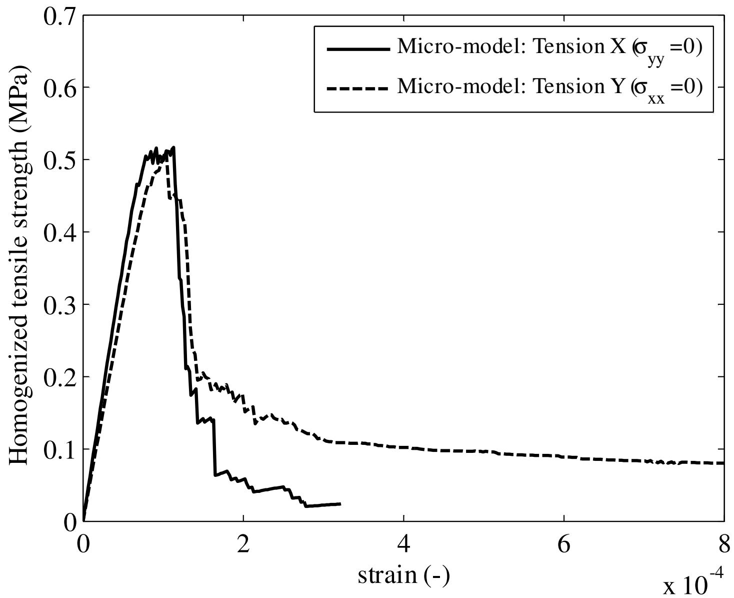

(a)

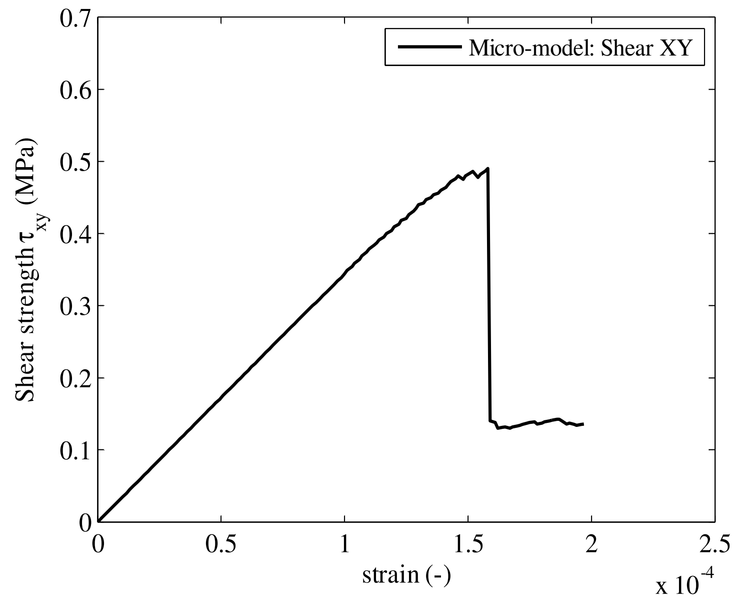

(b)

- Quasi-isotropic behavior in elasticity and plasticity.
- Homogenized tensile and shear strength governed by mortar joints.

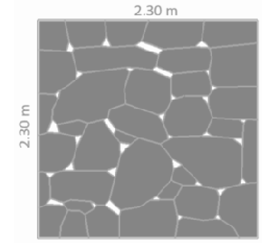

Rubble wall: 2D failure surfaces

One-step versus Two-step approach

- A 2D strength surface is provided (σ_{xx}, $\sigma_{yy}, \tau_{xy} = 0$); it is suitable for a plane-stress analysis.
- The difference between the one-step approach and the two-step approach is negligible.

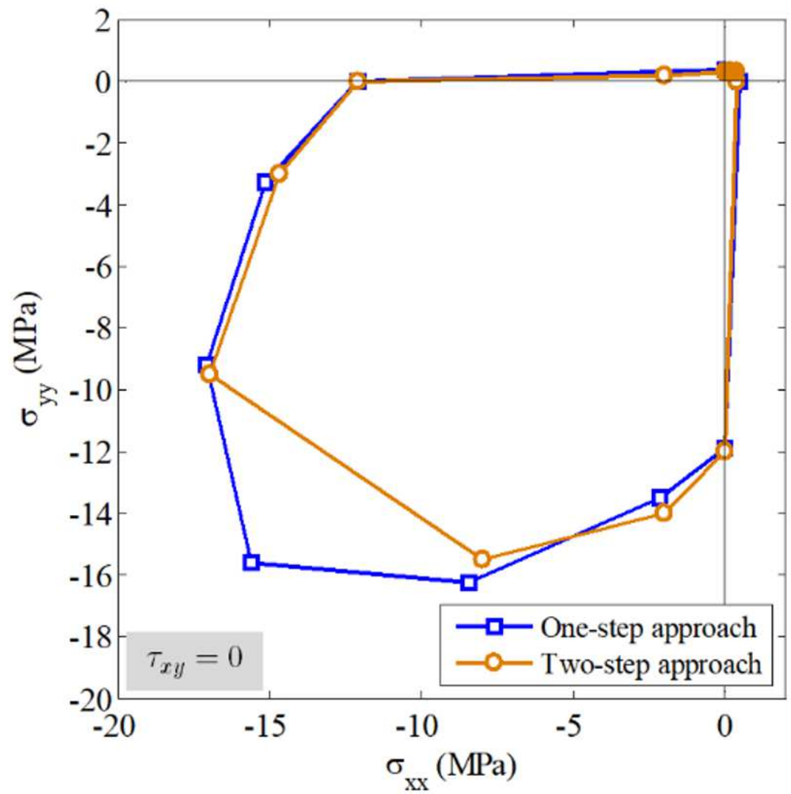

Rubble wall: 2D failure surfaces

One-step versus Two-step approach

- The **two-step** approach is far more time consuming that its counterpart.
- It poses some **numerical convergence issues**, especially for high stress values of pre-compression.
- It **hinders achieving the full envelope**.
- It was **unable to track segments AB and BC** since, in this region, a pre-compression value whose value can be higher than the uni-axial failure stress is required.

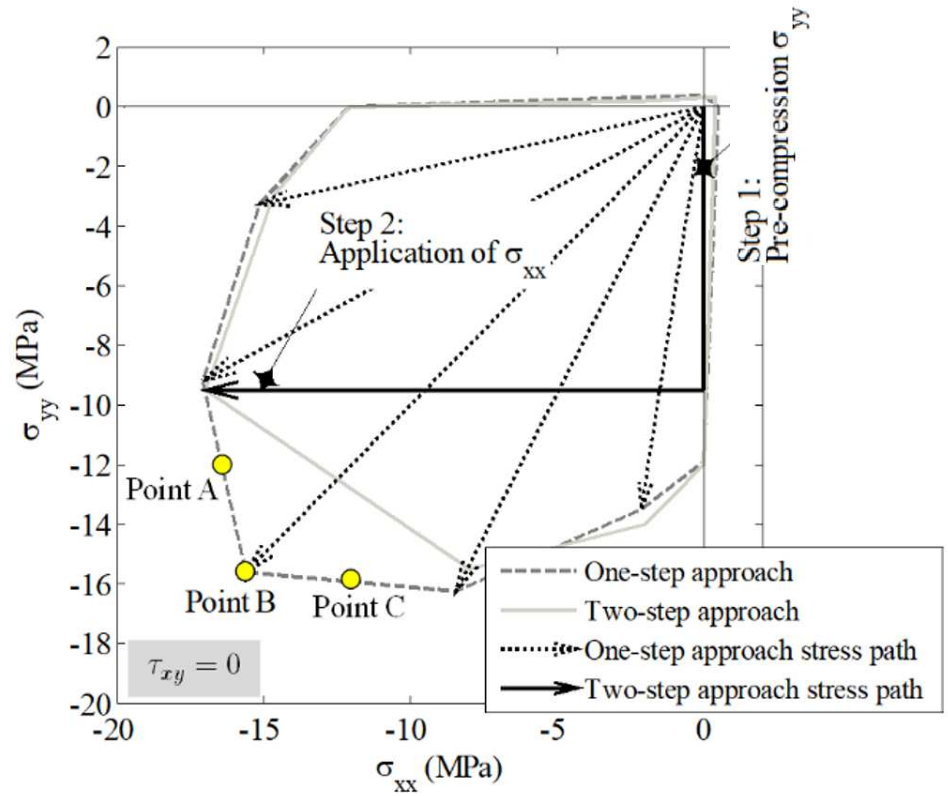

Rubble wall: 2D failure surfaces

One-step versus Two-step approach

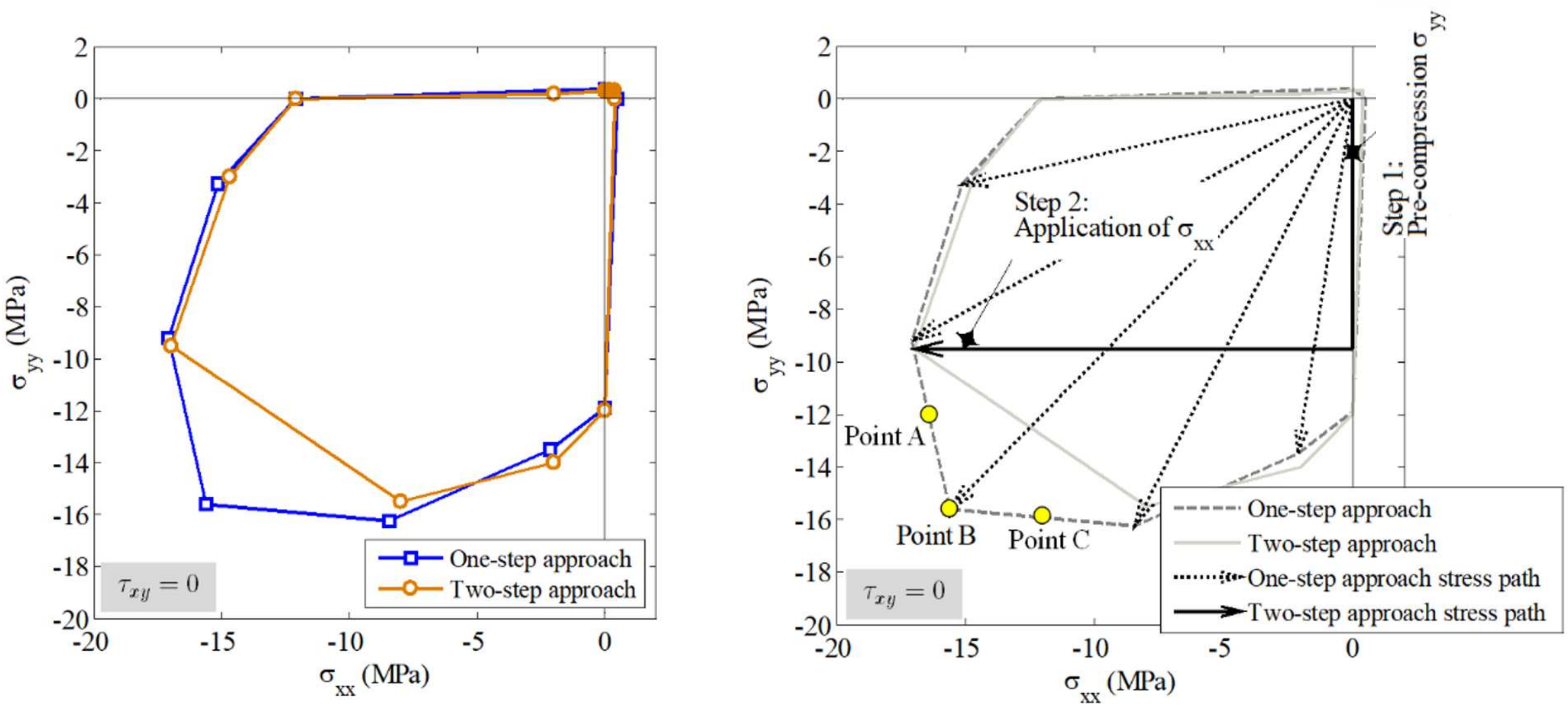

- For the considered rubble wall, the one-step approach is more suitable than its counterpart.
- This conclusion is to be confirmed by comparing the two approaches for other types of masonry walls.

Rubble wall: 3D failure surface (One-step approach)

- A 3D strength is provided ($\sigma_{xx}, \sigma_{yy}, \tau_{xy}$); it is suitable for masonry walls subjected to different states of stresses (axial and shear stresses).

- It shows a quasi-isotropic failure.
- Additional simulations are required aiming to smooth the surface.
- The lower part of the surface needs to be completed by applying a negative shear stress.

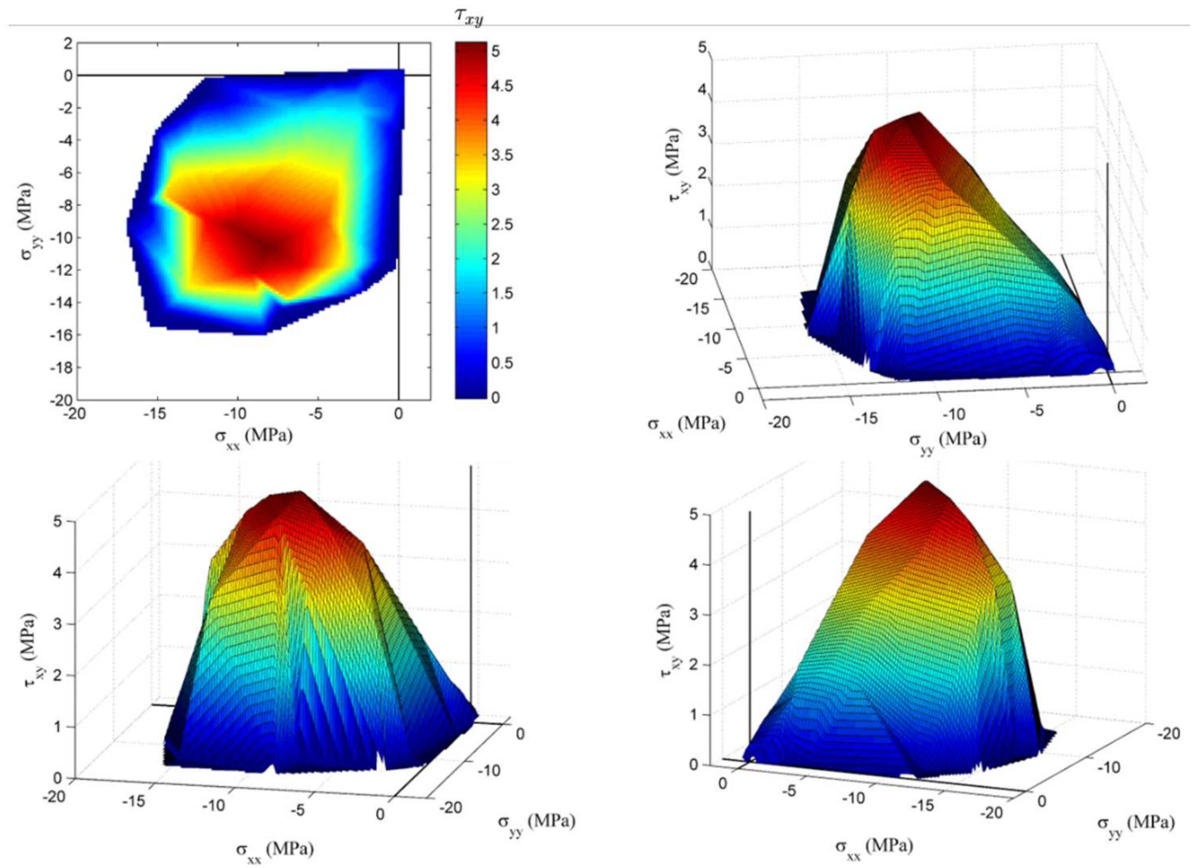

Two historic masonry bridges in Lebanon

Two masonry bridges - Lebanon

- Lebanon has a rich cultural heritage value that stands on 5000 years of history.
- **No structural studies can be found in the literature concerning masonry bridges in Lebanon.**
- **Two coastal masonry bridges are considered**.
- A preliminary structural assessment is performed through nonlinear pushdown and mass push-over analysis.
- A simplified micro-model is performed under plane stress conditions.

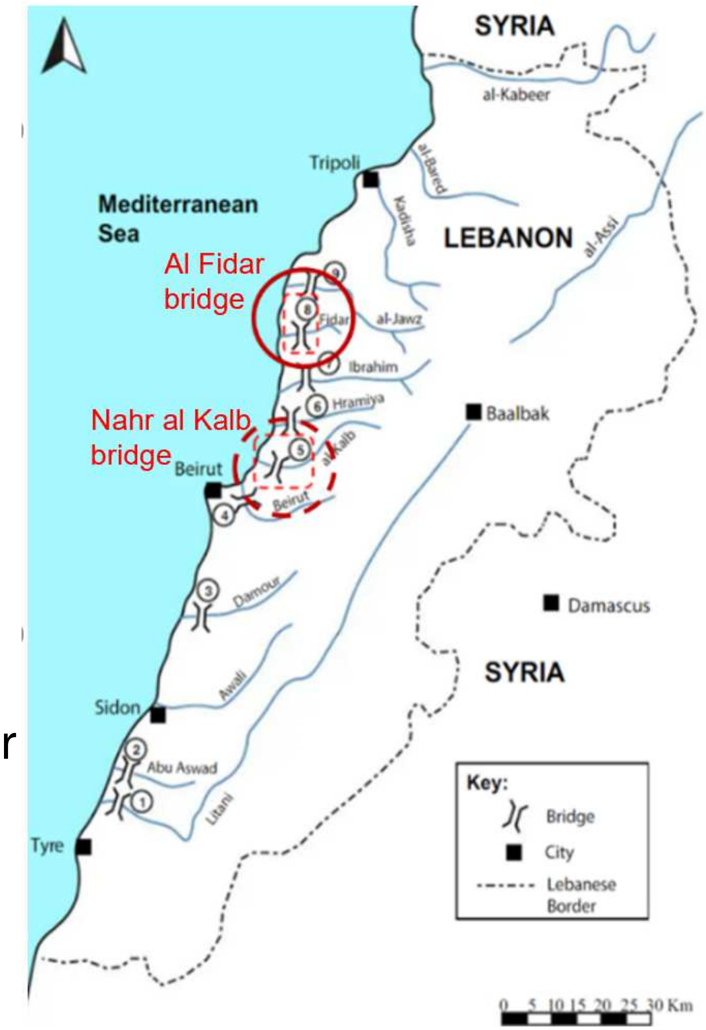

Two masonry bridges - Lebanon

Reliable structural assessment of masonry bridges

- Material characterization.
- NDT.
- Moving load.
- Supports settlement.
- Time history analysis.
- 3D modeling.
- Etc.

Out of the scope of the present work

Nahr Al Kalb Bridge

Nahr Al Kalb bridge

- The old bridge of Naher al Kalb is an iconic monument in Lebanon.
- It dates back to the Ottoman period (first mention **1344**).
- It suffers from **multiple disorders** principally due to **lack of maintenance**.

Nahr Al Kalb bridge

Geometry

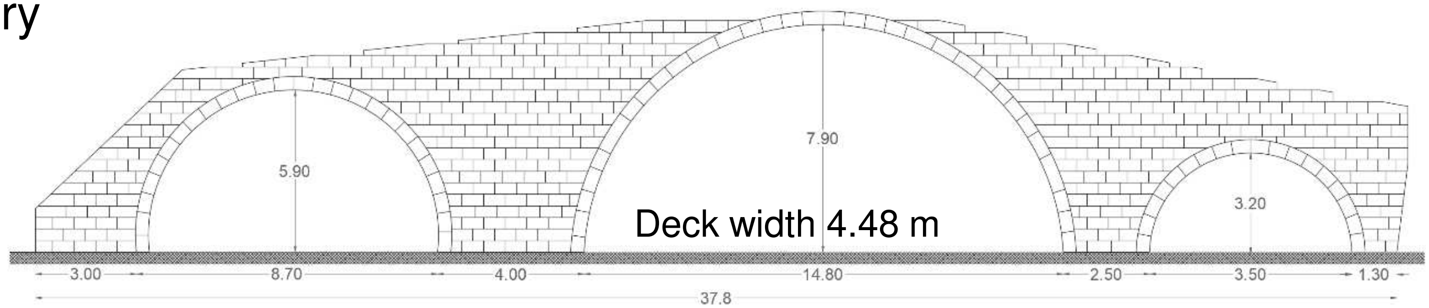

Materials

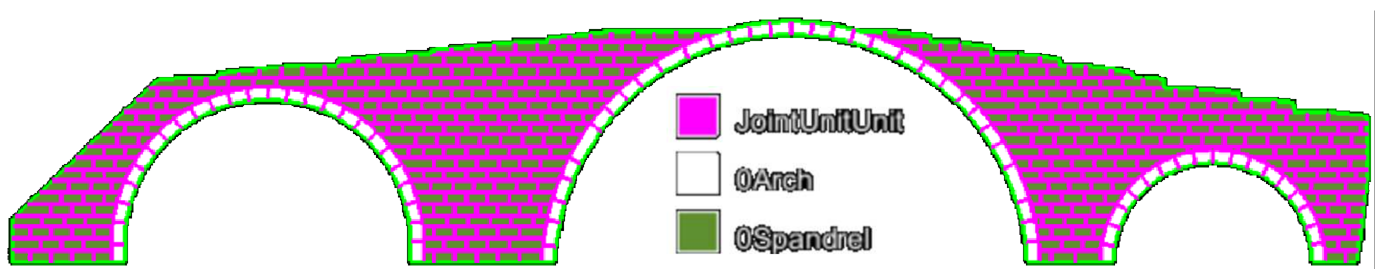

- *Units:* E_{brick} = 30,000 MPa; ν_{brick}=0.25; f_{cb} = 17 MPa, f_{tb} = 2 MPa, C_b = 5 MPa; Φ_b = Ψ_b =30 °; η_c = 0.7; η_ϕ = 0; B = 50; M = 0 *(brittle material).*
- *Mortar joints:* K_n = 25000 MPa/m; K_{0n} = 3000 MPa/m; K_t = 5000 MPa/m; K_{0t} = 1000 MPa/m; c = 0.05 MPa; f_{tm} = 0.05 MPa, $\phi = \psi$ = 25 °; e = 20 mm, h_r = 0.8; β = 1.1 (slightly brittle); β'=1.

Nahr Al Kalb bridge

Mesh and boundary conditions

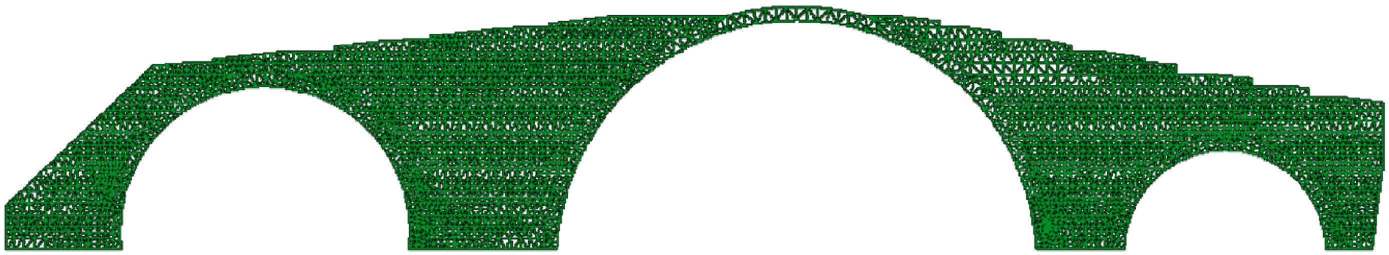

Vertical and horizontal displacements blocked under the supports, lateral edges released in the horizontal direction.
3367 nodes, 6212 triangular elements, 3079 zero-thickness interface elements.

Basic validation of the model

Vertical stress due to self-weight

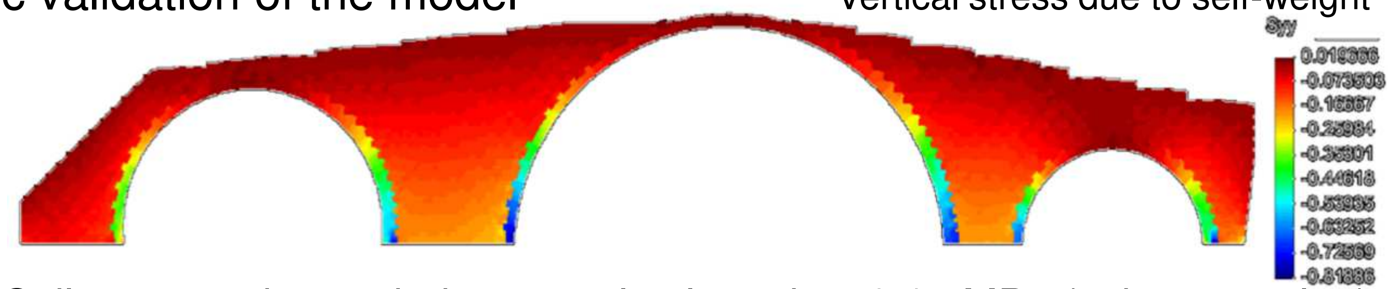

- Soil pressure beneath the central column is ≅ 0.17 MPa (coherent value).
- The river bed appears to have an acceptable bearing capacity.
- Maximum compressive stress is observed in the arche.

Nahr Al Kalb bridge: Pushdown analysis

Joint damage and failure mechanism

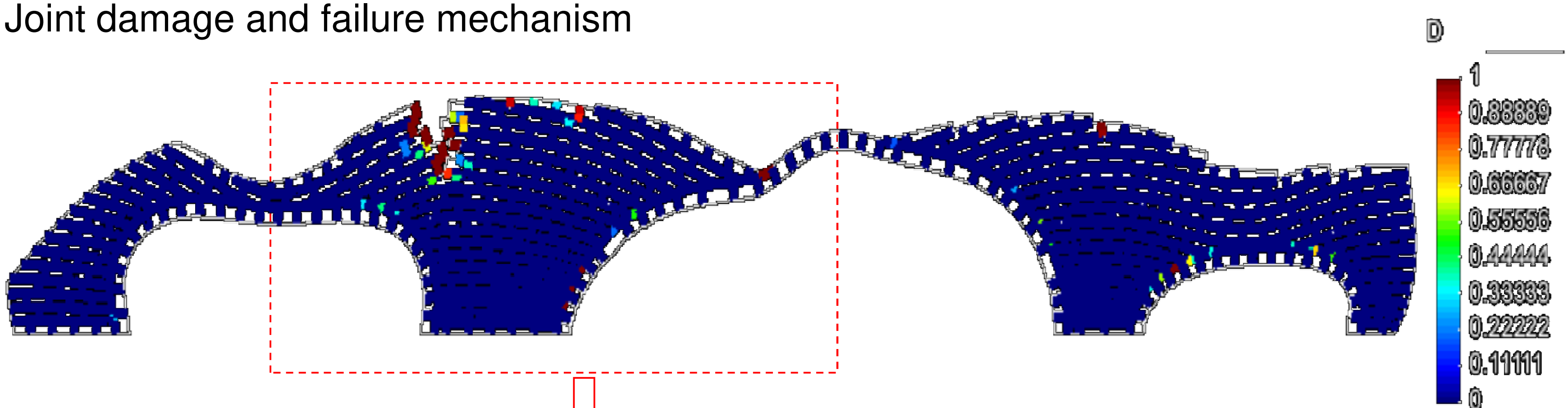

Parameters to be checked

- Mortar joint opening
- Vertical displacement

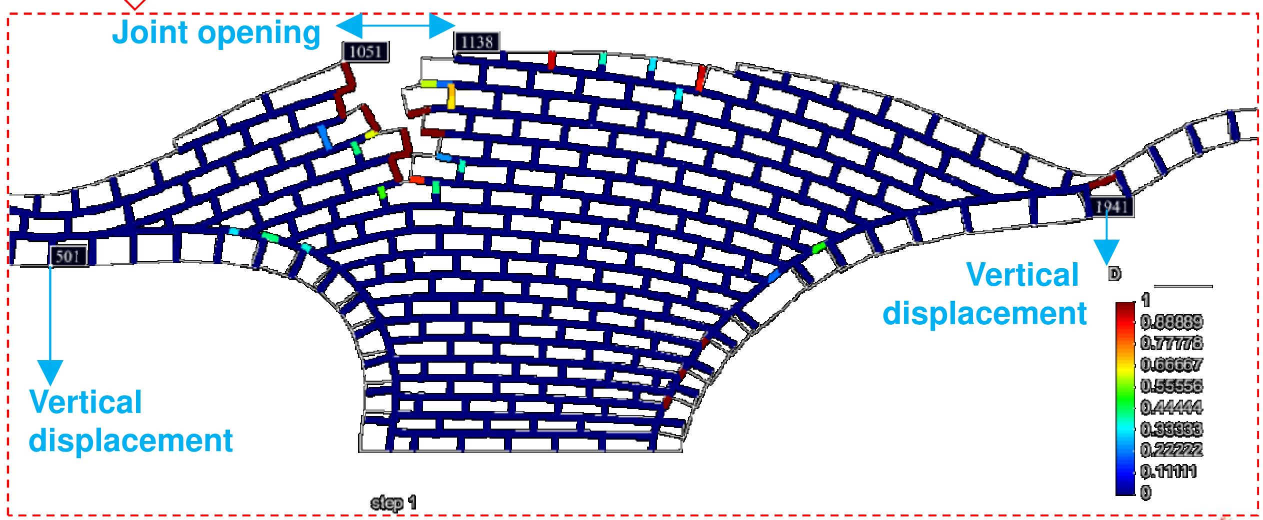

Nahr Al Kalb bridge: Pushdown analysis

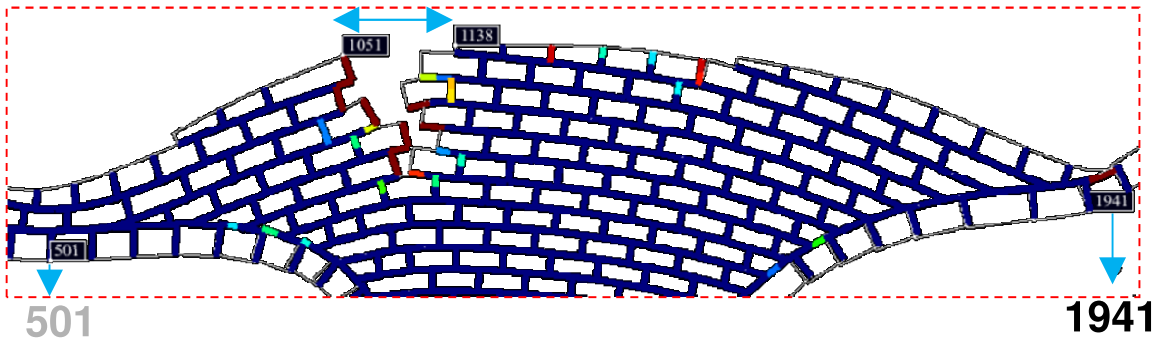

Vertical displacement: Node 501 and 1941.

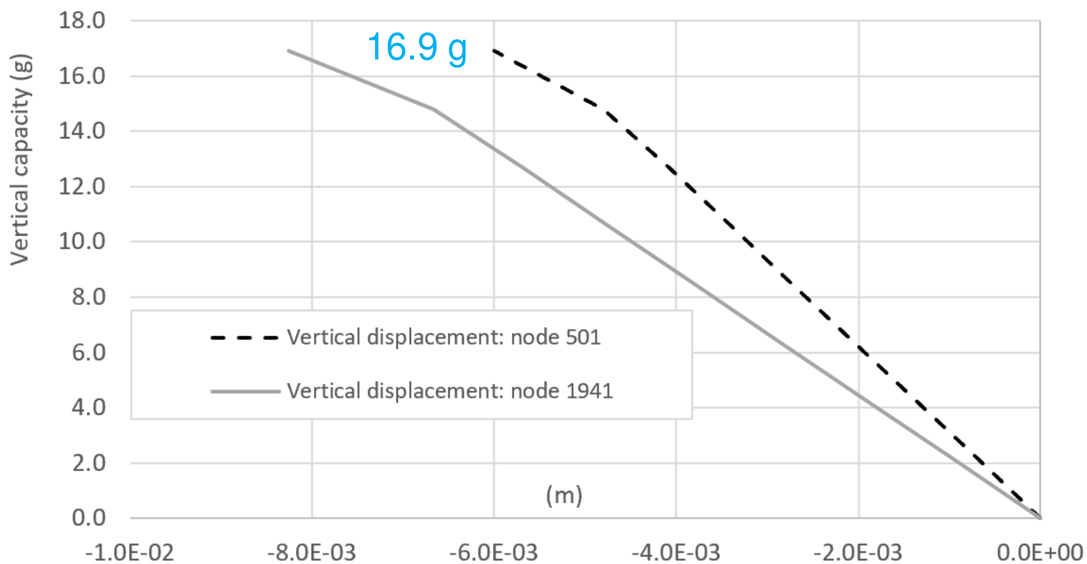

Nahr Al Kalb bridge: Pushdown analysis

Joint opening

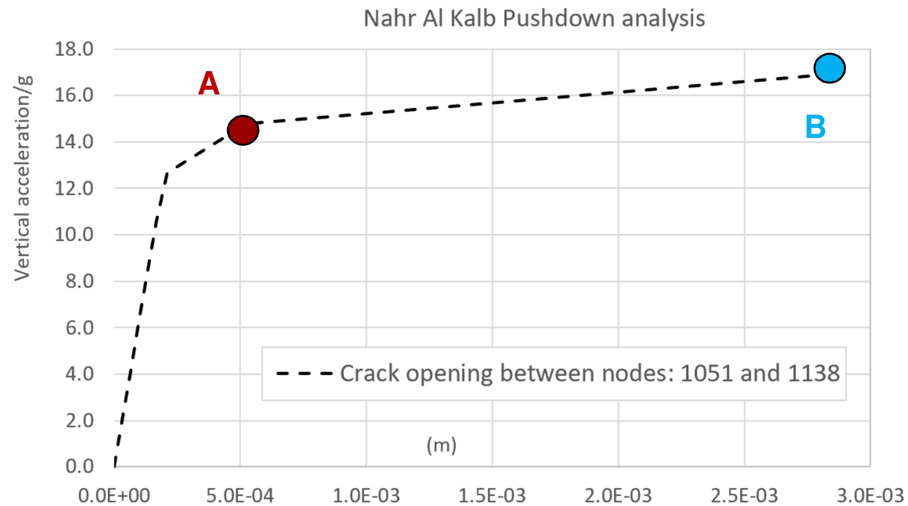

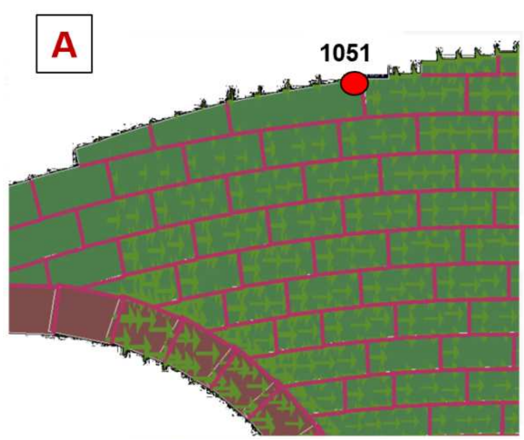

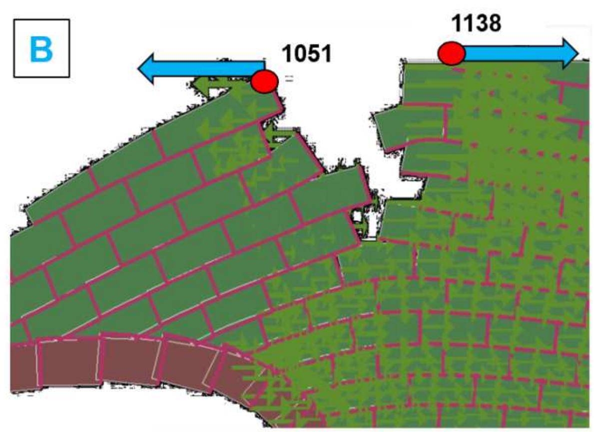

Nahr Al Kalb bridge: Pushover analysis

+X direction

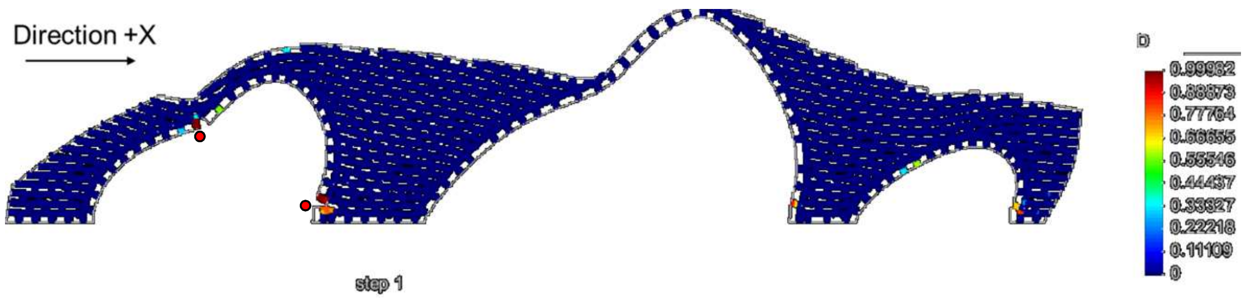

Damage in joints

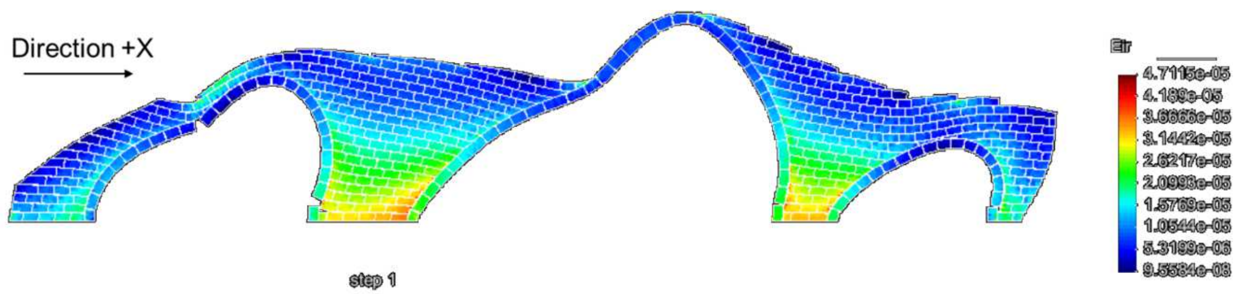

Irreversible strain

- A four-hinge failure mechanism is observed with a plastic hinge at the top left of the central keystone and above the base of the central pillar.

Nahr Al Kalb bridge: Pushover analysis

-X direction

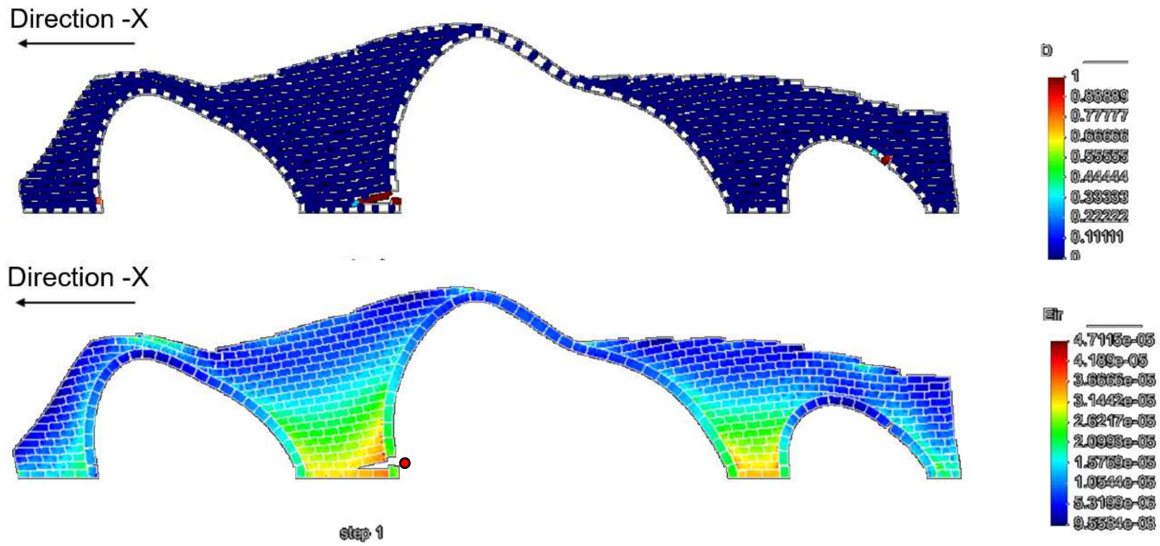

Damage in joints

Irreversible strain

- The failure mechanism is triggered at the base of the central left column due to an uplift effect and due to tension failure in the mortar bed joints.
- The right arch is affected by the onset of a plastic hinge on the right side of its central keystone.
- Irreversible strains are localized at the base of the central columns

Nahr Al Kalb bridge: Pushover analysis

+X direction

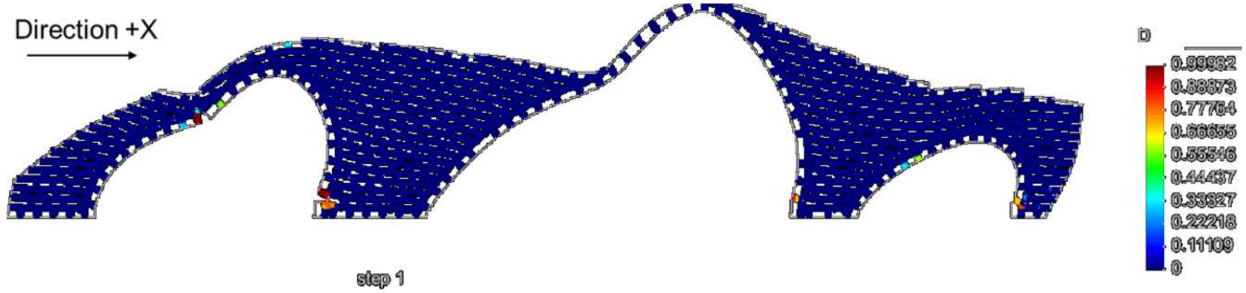

- The capacity value is 0.91g (considered as high).
- The response after cracking is more developed than Al Fidar bridge.
- Result can be more improved to have more insight on the strength and post-peak behaviour.

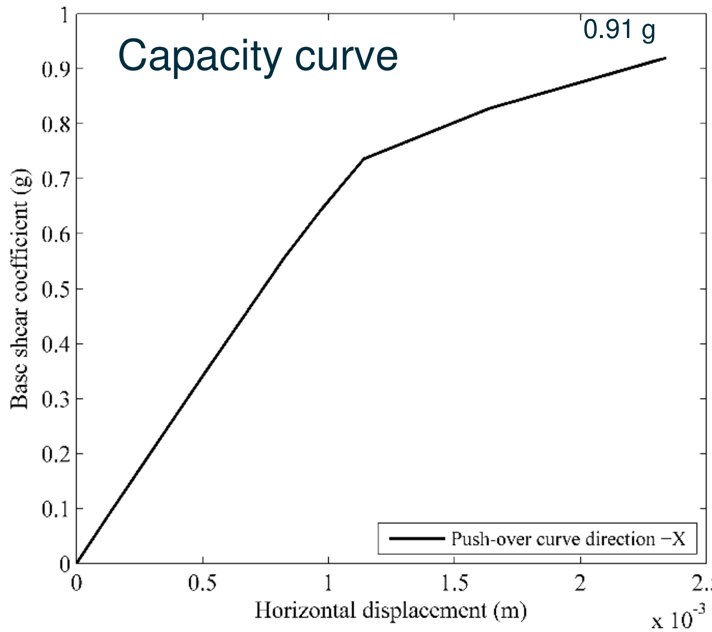

Nahr Al Kalb bridge: Macro-model

REV size

- Window test approach
  [Lourenço et al. 2013].
- 1.4x1.4 m^2 .
- 2.4x2.4 m^2.
- Rotation 45°.

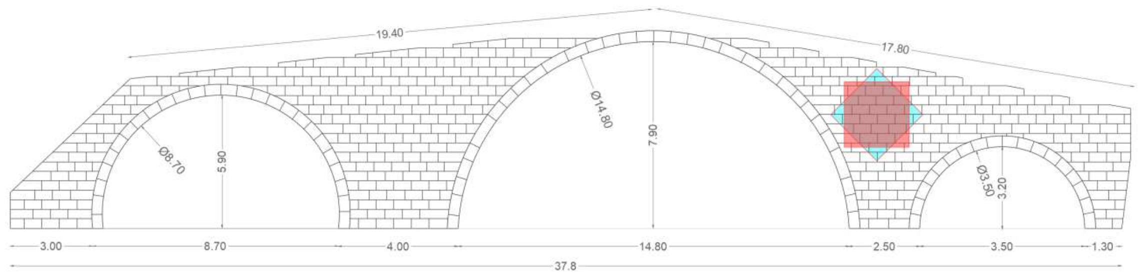

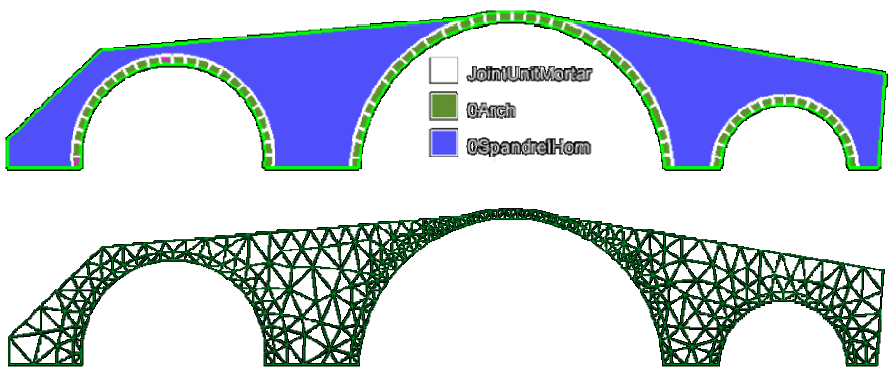

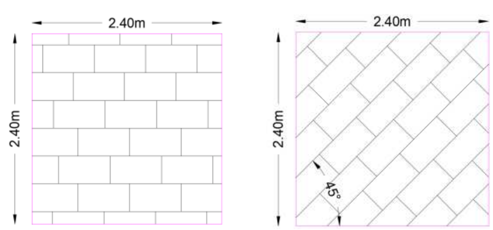

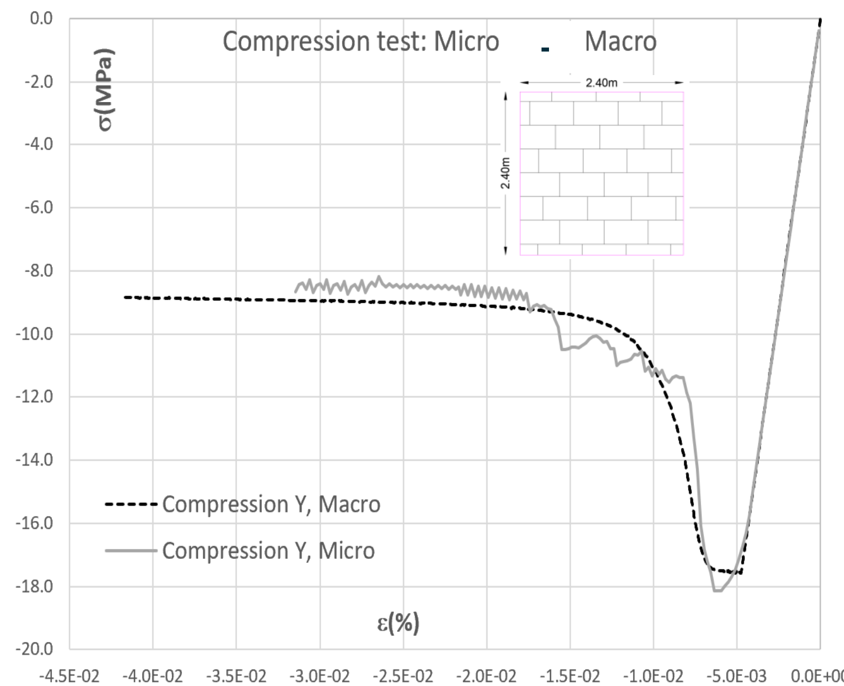

Nahr Al Kalb bridge: Macro-model

Vertical stress σ_{yy} due to self weight

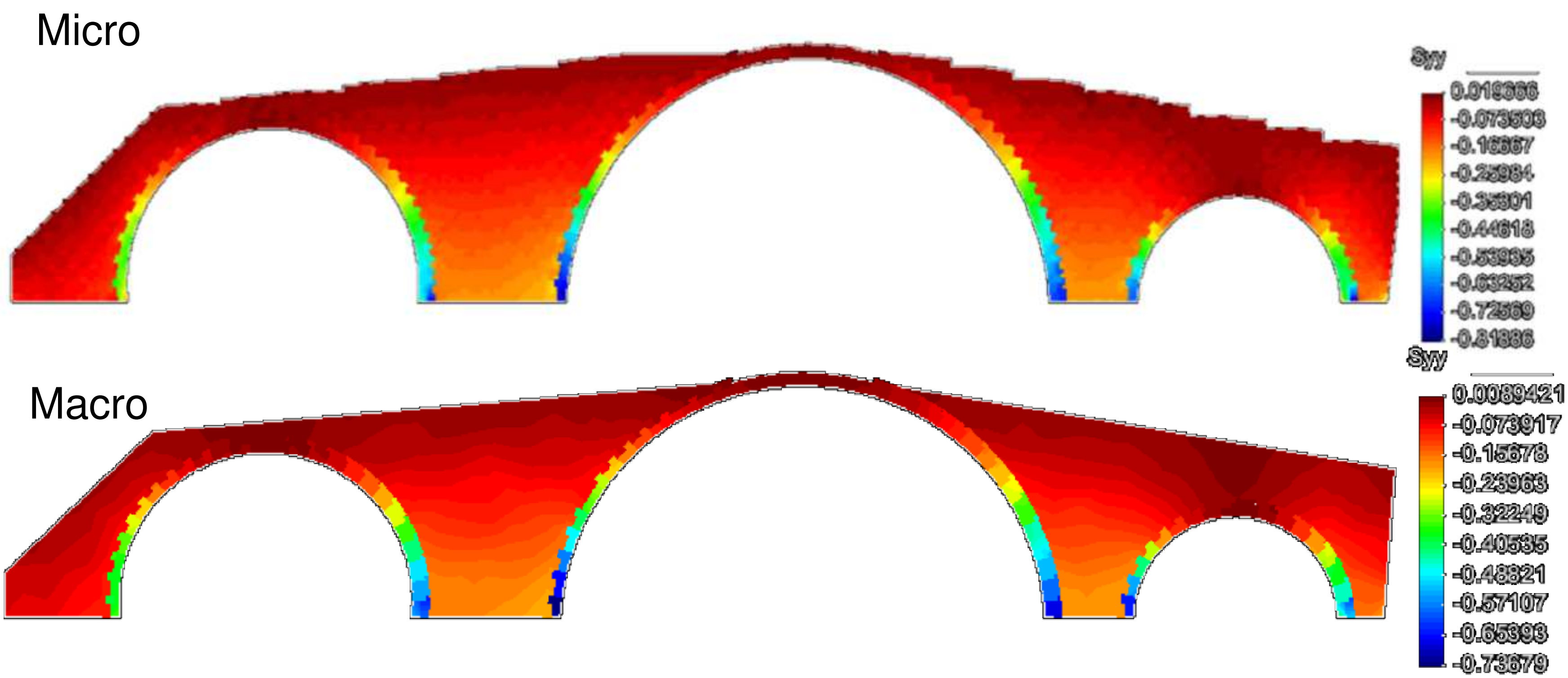

- Quasi-similar mapping distribution and stress values in spandrel walls and arches.

Al Fidar bridge

Al Fidar bridge

- The historic bridge was built over Al Fidar river. In **1292**, it was the location of a famous battle between Kurdish Muslim troops and local Christian forces [Petersen 2020].
- It is a **double arch irregular masonry bridge**, still operational nowadays.
- **Poorly maintained**.

Al Fidar bridge

Geometry

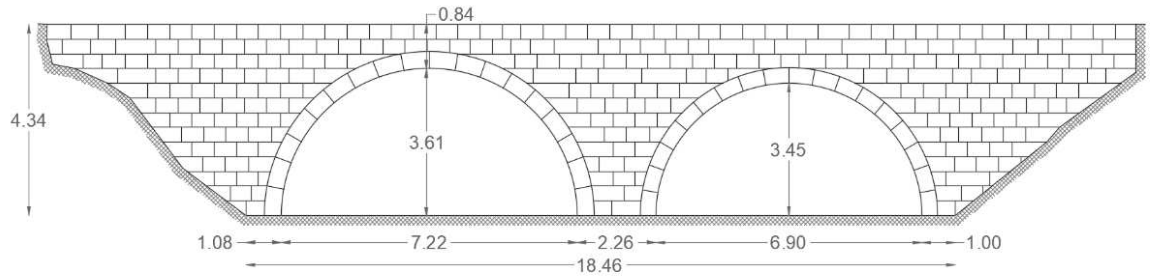

Materials

- The **mechanical properties** adopted for the masonry components rely on **empirical judgement** (lack of mechanical material characterization).

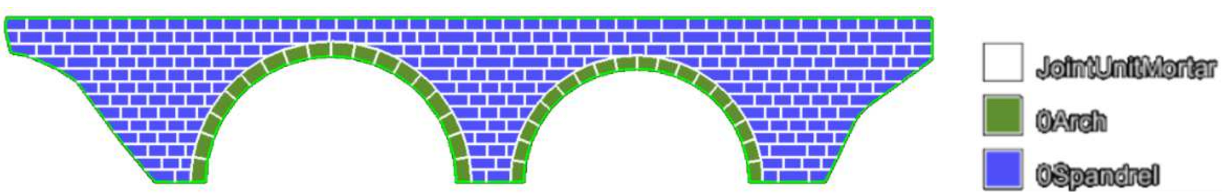

- *Units*: E_{brick} = 30,000 MPa; ν_{brick}=0.25; f_{cb} = 17 MPa, f_{tb} = 2 MPa, C_b = 5 MPa; Φ_b = Ψ_b =30 °; η_c = 0.7; η_ϕ = 0; B = 50; M = 0 *(brittle material)*.
- *Mortar joints*: K_n = 25000 MPa/m; K_{0n} = 3000 MPa/m; K_t = 5000 MPa/m; K_{0t} = 1000 MPa/m; c = 0.05 MPa; f_{tm} = 0.05 MPa, $\phi = \psi$ = 25 °; e = 20 mm, h_r = 0.8; β = 1.1 (slightly brittle); β'=1.

Al Fidar bridge

Mesh and boundary conditions

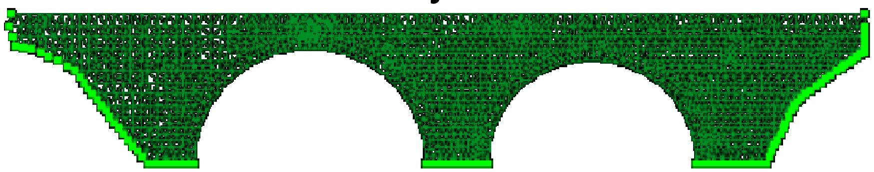

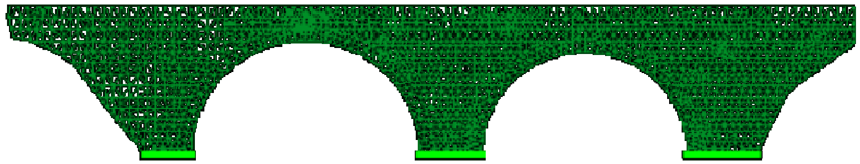

Vertical displacement blocked

Horizontal displacement blocked

(1959 nodes, 3619 triangular elements, and 1778 interface elements)

Basic validation of the model

Vertical stress due to self-weight

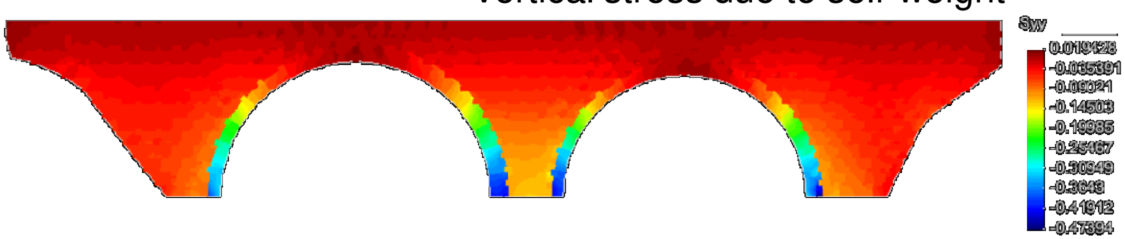

- Comparing the self-weight analysis and evaluate the vertical reactions.
- Soil pressure beneath the central column ≅ 0.1 MPa (coherent value).

Al Fidar bridge: Pushdown analysis

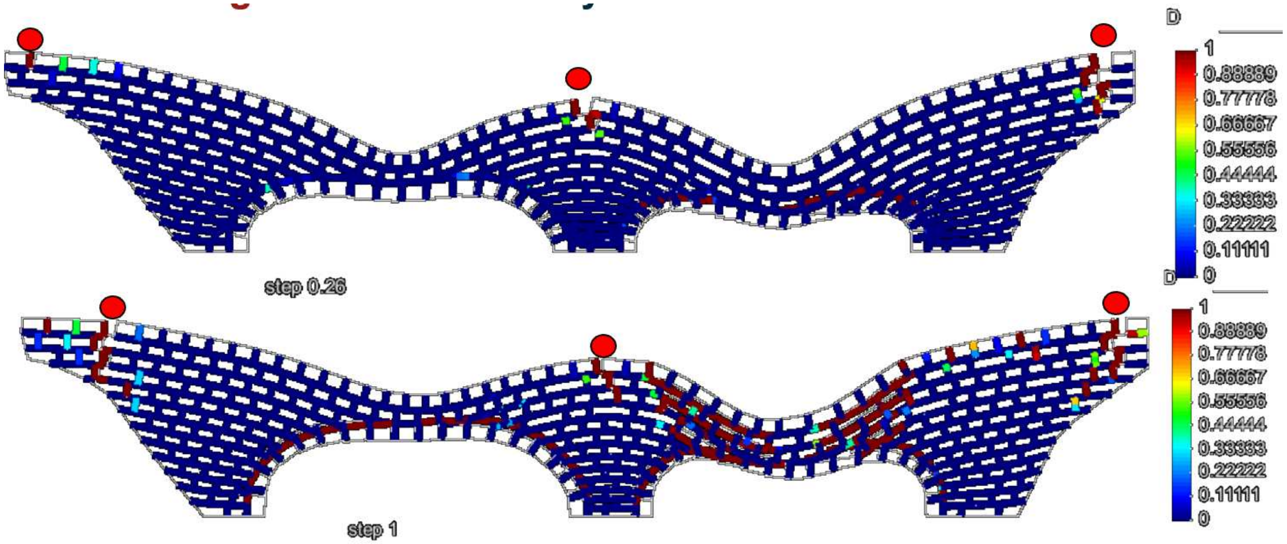

video

- Damage is initiated in the spandrel head joints above the supports (step 0.25), then in the joints between the arches and the spandrel units.

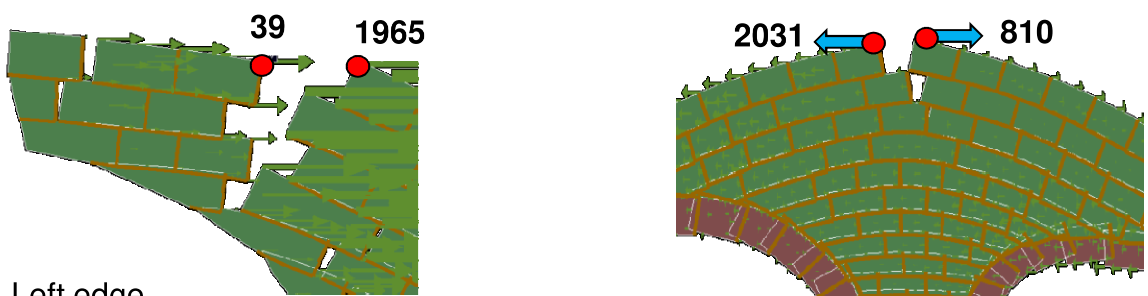

Left edge

Central column

Al Fidar bridge: Pushover +X direction

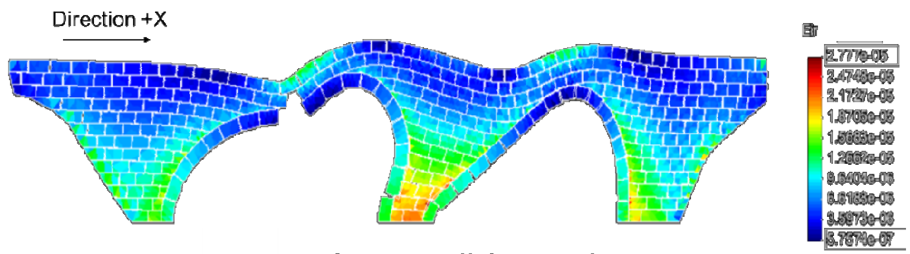

Irreversible strain

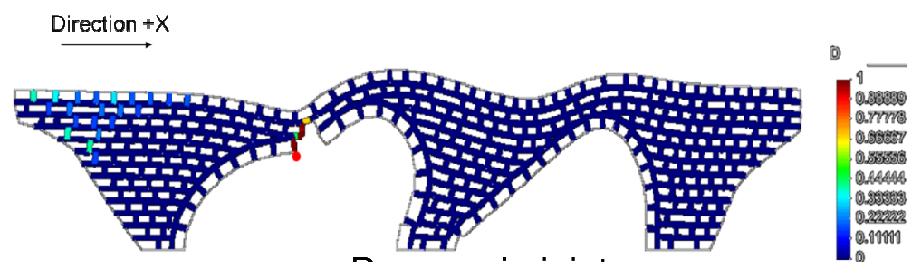

Damage in joints

- A **four-hinge failure mechanism** is observed in the left arch due to damage of mortar joint at the left side of the central keystone and near the base of the central column.
- At the right arch, a three-hinge mechanism is observed, and damage on some head-joints of the spandrel walls.
- The damage in the head joints above the left arch is due to joints tension stress.
- A **high irreversible** strain is **localized at the base of the columns** and on the spandrel area above the central keystone of the arches.

Al Fidar bridge: Pushover +X direction

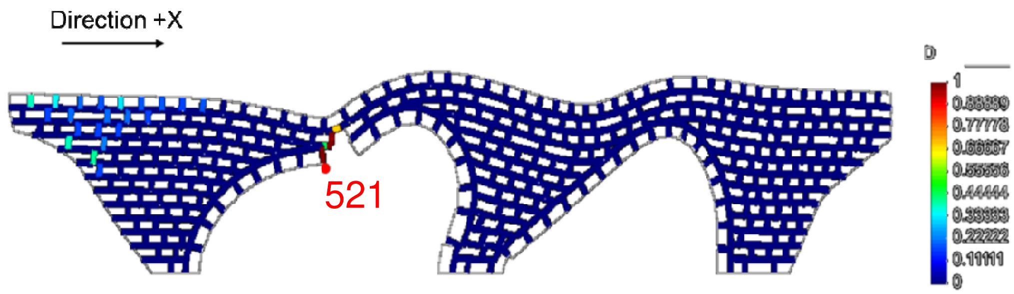

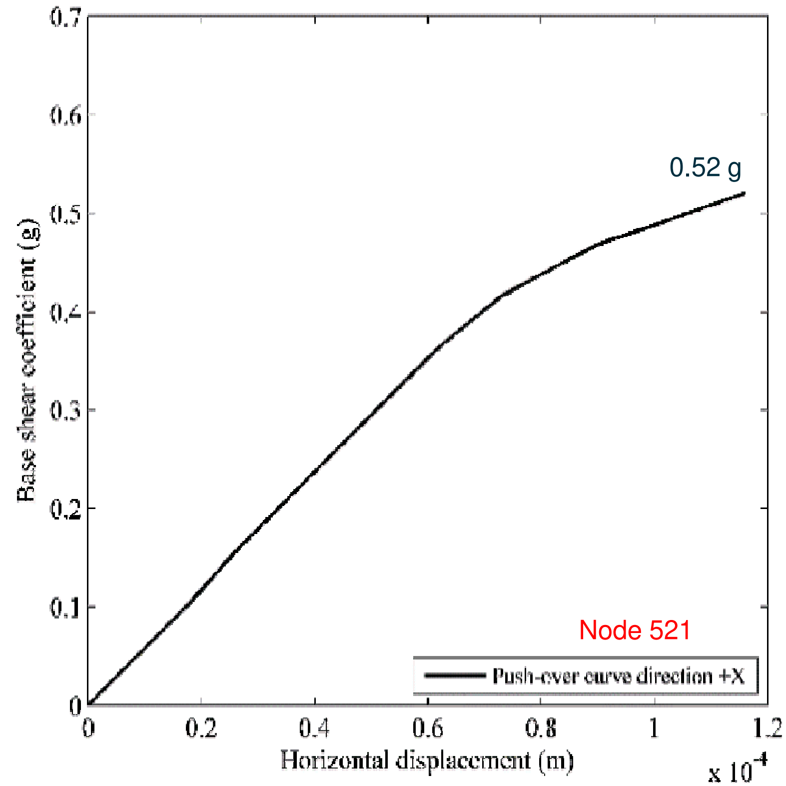

- An i7-8650U processor laptop has been used with 16 GB of memory RAM.
- The processing running time is 56 seconds.
- It is considered as very low computational time, but may be seen together with the low value of load increments (50 load increment).

Al Fidar bridge: (Micro-Macro)

Self weight

- Quasi-similar mapping distribution and stress values in the arches and spandrel walls.

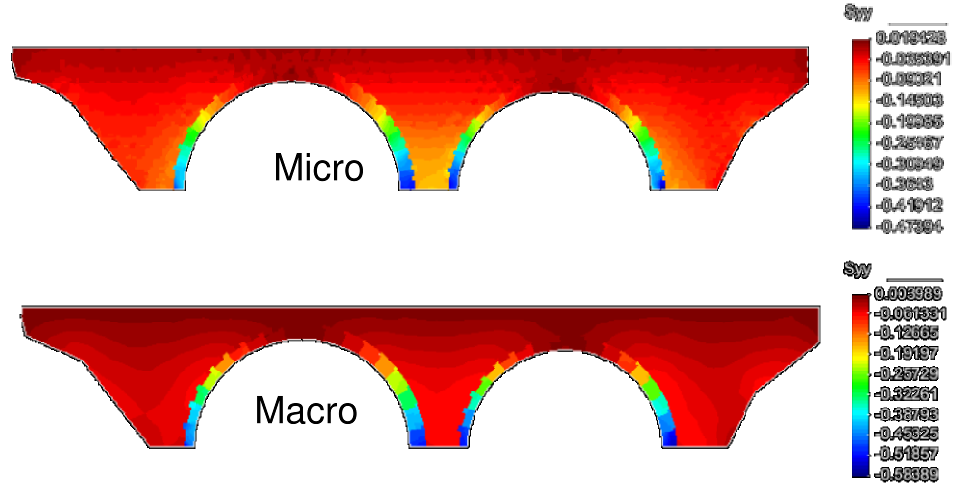

Pushover +X

- Comparable deformation shapes.
- Macro: Joint damage is distributed in the extrados of the left lower parts of each arch.

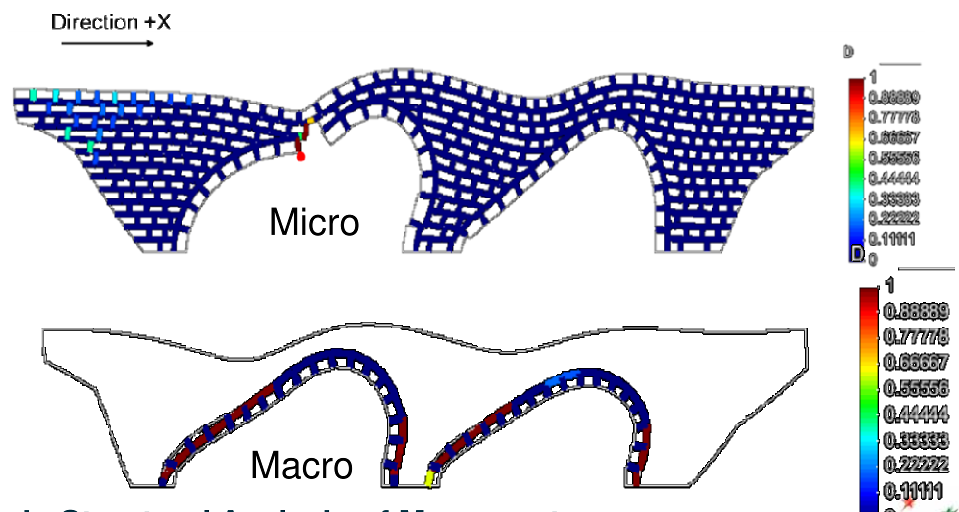

Al Fidar bridge: (Micro-Macro)

Pushover +X

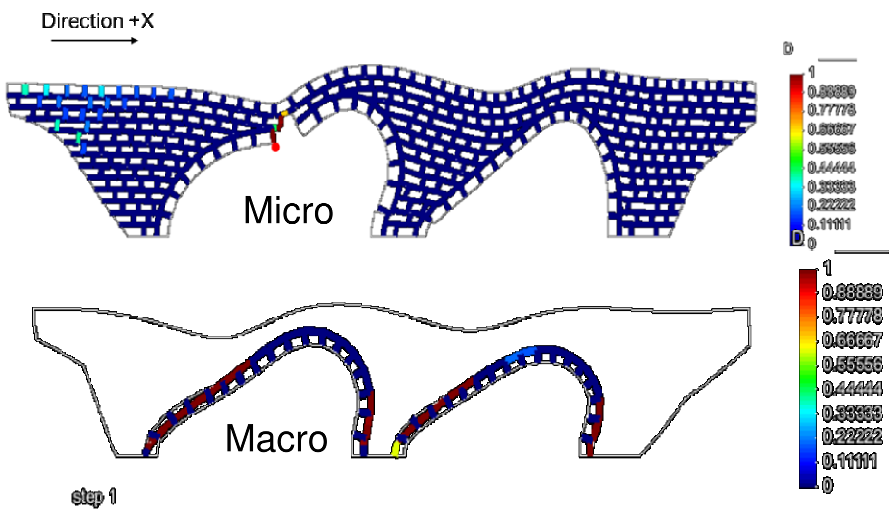

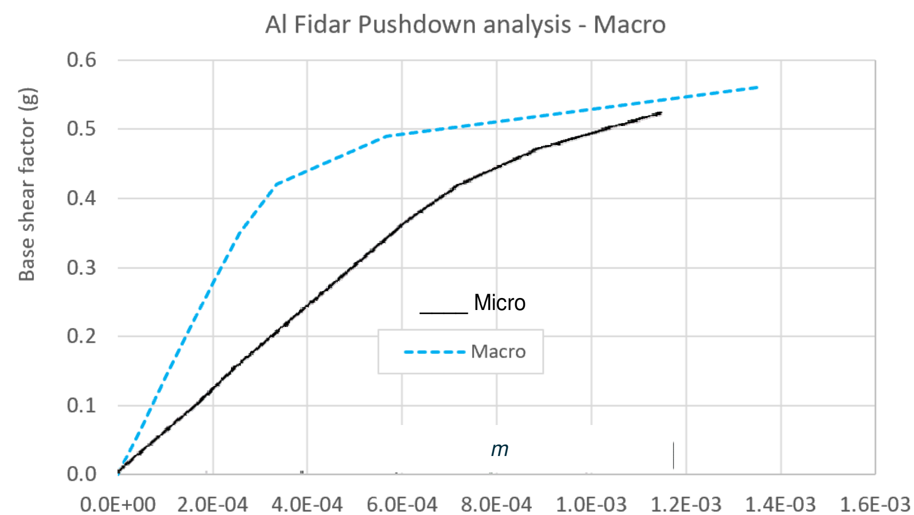

- Capacity : *0.52g Micro* versus *0.57g Macro.*
- The macro-model shows a stiffer response, this is due the assumption of the shear modulus (ellipsoidal elasticity).

Final remarks

Final remarks

- A **homogenization FE-based strategy** is presented with an emphasis on the applied boundary conditions.

- **Simplified Micro-scale model**

  - ➢ Unit-unit and unit-mortar interfaces are represented through zero-thickness interface with cohesive behavior with damage-plasticity and unilateral contact. Units are characterized by an orthotropic behavior in the elastic phase and an anisotropic plastic behavior with softening.

  - ➢ The validation of such micro-scale approach has been conducted on a **running-bond** masonry wall, for in-plane compression tests and in-plane and out-of-plane shear and tension tests.

Final remarks

- **Macro-model**

  - The formulation of a new **anisotropic macro-model** (ANELVIP) **with softening** is presented.
  - Validation tests on Flemish-bond masonry wallets have confirmed the **accuracy** of the macro-model **in compression** - both in elastic and inelastic ranges.
  - The overestimation of the shear modulus due to the ellipsoidal elasticity assumption has been solved by introducing an independent shear modulus parameter as a direct input.
  - The **shear peak** value and **residual stress** are **accurately represented**.
  - The macro-model can reproduce the homogenized tension Young's moduli (directions x and y) and the peak stress. The ongoing validation of the new developed **softening in tension** shows promising results.

Final remarks

- An algorithm is developed to cope the difficulties related with the FE pre-processing stage of a structure with **high density of joints**.
- Case study 1: a **rubble wall**
  - Good efficacy to: obtain the homogenized stress-strain curves; to predict the failure mechanism; and to generate the composite strength domain (2D and 3D).
  - The difference between the two-step and one-step strategy strategies is negligible. **The one-step loading** path strategy **is more practical** from an engineering standpoint (for the considered wall).
- Case study 2: **Two masonry bridges**
  - The case studies allowed to apply the developed numerical models and **predict the expected failure mechanisms** of structures with **high density of fractures**.
  - The computational application is promising due to the **low computational time cost**.

Final remarks

➢ The obtained results of the pushdown and pushover analysis should be examined within a qualitative approach due the lack of materials mechanical characterization.

Perspectives of the present work

- ANELVIP macro-model : Validation of the new version in shear (independent shear modulus), and tensile behavior (with softening).

31430 ANELVIP: Anisotropic ElastoViscoPlasticity Mohr-Coul.(0)/Druck.-Prag.(1,2,3)+ Creep

Nb: 24

Param1 = E_1	Param13 = $b^p{}_T$
Param2 = E_2	Param14 = a
Param3 = ν_{12}	Param15 = n
Param4 = ν_{13}	Param16 = α
Param5 = μ_{12}	Param17 = σ_c
Param6 = ω (in degrees)	Param18 = $a^v{}_N$
Param7 = C	Param19 = $b^v{}_T$
Param8 = ϕ (in degrees)	Param20 = ε_0
Param9 = ψ (in degrees)	Param21 = η_c
Param10 = σ_T	Param22 = η_ϕ
Param11 = *Option* (01,2,3)	Param23 = B
Param12 = $a^p{}_N$	Param24 = M

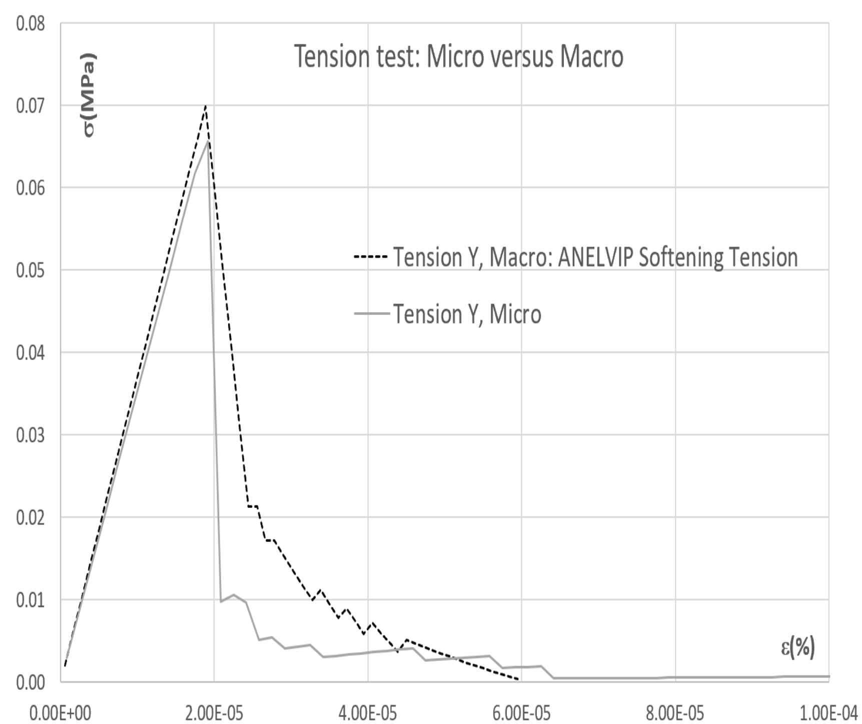

Perspectives of the present work

- Extension of the proposed homogenization approach to **other types of masonry** through a statistical approach: a **database** may result offering anisotropic mechanical parameters and strength surfaces.
- Refined **calibration** of the bridges macro-model: Additional simulations should be conducted considering different types of loading (***concentrated***, moving, etc.)
- Engineering applications: The applied FE approach (micro- and macro-) may be of a practical use for a structural assessment of masonry structures.

Chalhoub M (2006) Apports des méthodes d'homogénéisation numériques à la classification des massifs rocheux fracturés (PhD thesis, in French). Ecole Nationale des Mines de Paris, Mines ParisTech

Chalhoub M (2010) Massif rocheux: Homogénéisation et classification numériques. Presses des Mines, 2010, 232 pages, Paris

Chalhoub M, Pouya A (2016) Modélisation du renforcement des ouvrages en maçonnerie par la méthode des éléments finis : Etude de deux cs du patrimoine libanais bâti. In: JNM2016. IFSTTAR Ecole des Ponts, ParisTech, 17-18 Mars 2016.

Disroc (2020) A Finite Element Code for modelling Thermo-Hydro-Mechanical processes in fractured porous media -Catalog of Materials (http://www.fracsima.com/DISROC/Materials-Catalog.pdf).

DISTRUCT (2020) DISTRUCT Solutions s.a.r.l., company profile. www.distruct.com

Petersen A (2020) Roman, Medieval or Ottoman:Historic Bridges of the Lebanon Coast. Bridg Civiliz 175–203

Pouya A, Ghoreychi M (2001) Determination of rock mass strength properties by homogenization. Int J Numer Anal Meth Geomech 25:1285}1303. doi: 10.1002/nag.176

Pouya A (2007) Ellipsoidal anisotropies in linear elasticity, Extension of Saint Venant's work to phenomenological modelling of materials. J Damaged Mech 16:95–126

Pouya A, Chalhoub M (2008) Numerical Homogenization of Elastic Behavior of Fractured Rock Masses and Micro-cracked Materials by FEM. In: IACMAG. Goa, India, pp 403–407

Thank you for your attention